

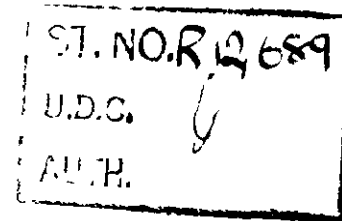
C.P. No. 183



C.P. No. 183

(16,578)

A R C Technical Report



MINISTRY OF SUPPLY

AERONAUTICAL RESEARCH COUNCIL

CURRENT PAPERS

An Analysis of N.A.C.A. Helicopter Reports

By

Captain R N Liptrot, C.B.E., B.A.

LONDON HER MAJESTY'S STATIONERY OFFICE

1954

SIX SHILLINGS NET

R 12,689

22 APR 1955

4 NOV 1955

20 JAN

3 8006 10038 0396



C.P. No. 183

Report No. RD/H/2

MINISTRY OF SUPPLY

RD/HELICOPTERS

An Analysis of N.A.C.A. Helicopter Reports

- By -

Captain R. N. Liptrot, C.B.E., B.A.

January, 1954

An Analysis of
N.A.C.A. Helicopter Reports

- by -

Captain R. N. Liptrot, C.B.E., B.A.

SUMMARY

Theory is compared with flight and model tests, in order to obtain empiric correcting factors which will enable reliable performance estimates to be made for new helicopter designs. A survey of general theory is followed by an analysis of certain American reports. Correcting factors for effective blade drag for tip speed ratio, compressibility and stalling of the retreating blade are derived. A method of calculating the retreating blade tip angle of attack for twisted blades is presented.

The work was carried out by the author under Ministry of Supply sponsorship.

LIST OF CONTENTS

		<u>Page</u>
1	Introduction	4
2	Methods of analysis	4
2.2	Induced velocity and induced power when hovering	4
2.3	Blade profile drag and profile drag power	8
2.4	Forward flight	11
2.4.1	Induced power in forward flight	11
2.4.2	Blade profile drag and profile drag power	13
2.4.3	Retreating blade tip angle of attack	14
2.4.4	Blade flapping angle and control to trim in forward flight	16
3	Analysis of American Reports	19
3.1	Hovering	19
3.11	N.A.C.A. Technical Note 626	19
3.12	Full scale tunnel tests on two 25' rotors	19

	<u>Page</u>	
3.13	Full scale tunnel tests on six rotors	19
3.14	Flight tests	20
3.15	Full scale tunnel tests on contra rotating coaxial rotors	22
3.16	Some theoretical investigations	22
3.161	Effect of rotor tip speed on hovering performance	22
3.162	Effect of blade profile drag characteristics on hovering performance	23
3.163	Effect of blade twist and plan-form taper on hovering performance	24
3.2	Full scale tests in forward flight	26
3.21	Tunnel tests	26
3.22	Flight tests	27
3.221	Variation in effective blade drag with forward speed	27
3.2211	Variation in effective blade drag with tip speed ratio, $(f)_\mu$	27
3.2212	Compressibility correction, $(f)_c$	27
3.2213	Stalling correction, $(f)_s$	29
3.3	Full scale tests on autorotative glides	30
3.4	The effects of blade twist	30
3.5	Blade flapping and control to trim	31
List of Symbols		33
List of References		37
Appendix		40

LIST OF TABLES

<u>Table</u>		<u>Page</u>
I	Coefficients in Nikolsky and Seckel expression for λ_{nf}	13
II	Comparative rotor power required to hover at sea level. Six rotors from tests in N.A.C.A. A.R.R. No. L5F25b	21
III	Vertical flight performance of a typical helicopter	23
IV	Effect of combined twist and taper on hovering performance	25
V	Increase in hovering thrust as compared with the thrust of an untwisted rectangular blade	26

1. Introduction

The work was sponsored by the Ministry of Supply, and one of the main objects in view was to compare theory with flight and model test results in order to obtain empiric correcting factors which would enable reliable performance estimates to be made for new helicopter designs, experience having shown that the methods already published, e.g., Talkin¹, Wald², Castles³, and Gustafson⁴ all underestimate the power required particularly at the higher speeds.

Some comparisons between estimates and measured performance have been given in an unpublished A.R.C. paper⁵.

2. Methods of Analysis

2.1 Although the various formulae used in the analysis have been published previously they occur in scattered reports, and some of them may not be generally known, or used, and it has been considered useful to collect them in this report for the convenience of others who may have to undertake similar analyses, and particularly for the growing body of students of aeronautics who are now meeting helicopter theory for the first time.

Except perhaps for the treatment of blade stalling and compressibility corrections there is little that is new.

A word of warning is necessary to those using existing reports from the various research organisations, since considerable confusion exists. Almost all the published work on helicopters is based on early autogiro theory, and the sign conventions of the autogiro theory have been generally maintained in American reports, where upward flow through the disc is taken as the positive sense, so that the inflow ratio λ will be negative for the helicopter in powered flight. Some more recent British reports take the helicopter inflow as the positive sense, so that when using formulae "lifted" from a publication care should be taken to examine the context, and to check the sign convention in use. As a corollary to this the sign of disc incidence should be watched, since with the autogiro convention disc incidence will be negative in the helicopter normal flight case, i.e., with disc tilted forward. Moreover, special care is necessary over incidence which in British reports is the attitude of the rotor disc to the relative wind, but in most American reports is the attitude of a plane at right angles to the no-feathering axis.

IN ALL CASES BEFORE APPLYING FORMULAE CULLED FROM A REPORT OR PUBLICATION REFERENCE SHOULD BE MADE TO THE LIST OF SYMBOLS, AND WHERE, AS IS OFTEN THE CASE, THE LIST IS NOT SPECIFIC AS TO SIGN CONVENTIONS REFERENCE SHOULD BE MADE TO THE CONTEXT OF THE FORMULAE AND TO ANY EXPLANATORY SKETCHES.

In order not to add to the existing confusion the American conventions are used throughout the present report, so that sign differences will be found between formulae used here and corresponding formulae to be found in some British publications.

2.2 Induced Velocity and Induced Power when Hovering

All analyses of blade mean effective drag depend critically on the estimate of induced power, and here we are in immediate difficulty since almost all published theory is based on the assumption of uniform induced velocity. By suitable twist it is of course possible to obtain constant induced velocity across the disc, but practical blades do not usually have this "ideal" twist. It is suggested that for routine estimates the usual formulae based on uniform induced velocity should be used with an empiric correcting factor.

We can obtain an idea of the order of such a correction for untwisted rectangular blades in the following way, by assuming, as is closely true (vide Ref. 6), that when hovering the induced velocity of an untwisted, constant chord, blade varies linearly from zero at the root to a maximum near the tip.

For/

For uniform distribution the induced power would be given by:

$$P_i = T \sqrt{\frac{T}{2\rho\pi R^2}} \quad \dots(1)$$

For the assumed triangular distribution the induced velocity v_r at any radius r will be given by

$$v_r = \frac{r}{R} \cdot v_t \quad \text{where } v_t \text{ is the induced velocity at the tip.}$$

Considering an annulus of the disc at radius r and width dr the thrust is given by:

$$\Delta T = (\rho 2\pi r \cdot dr \cdot v_r) 2v_r = 4\rho\pi r v_r^2 \cdot dr$$

$$\text{or } \Delta T = \frac{4\rho\pi v_t^2 \cdot r^3 \cdot dr}{R^2}$$

and integrating between the limits 0 and R.

$$T = \rho\pi R^2 v_t^2$$

whence

$$v_t = \sqrt{\frac{T}{\rho\pi R^2}} \quad \dots(2)$$

The induced power loss for the annular element is:

$$\begin{aligned} \Delta T v_r &= 4\rho\pi r v_r^3 \cdot dr \\ &= \frac{4\rho\pi r^4 \cdot v_t^3}{R^3} \cdot dr \end{aligned}$$

Integrating between the limits 0 and R the total induced power loss is

$$P_i = \frac{4}{5} \rho\pi R^2 \cdot v_t^3$$

and substituting for v_t from (2) we finally have

$$P_i = \frac{4}{5} \cdot T \cdot \sqrt{\frac{T}{\rho\pi R^2}} \quad \dots(3)$$

The ratio of the P_i from (3) to that from (1), i.e., the ratio of the induced power for an untwisted, constant chord blade to that for uniform induced velocity is thus $\frac{4}{5}\sqrt{2}$ or 1.13.

This/

This estimate however does not take into account the additional losses due to rotation in the downwash, which from Glauert⁷ can be taken as about 2% of the induced power for conventional rotor parameters, so that the overall correction can be taken as 1.15. Some reports, as for example Ref. 8 and Ref. 9, suggest a factor as high as 1.20 but 1.15 will be retained here as past experience, and the analyses made during the preparation of this report, show that this factor gives satisfactory hovering power estimates.

In general however in this report a separate allowance will be made for tip losses by introducing a tip loss factor B, which can be satisfactorily approximated as:

$$B = 1 - \frac{\text{tip chord}}{\text{radius}} \quad \dots(4)$$

For conventional plan forms, B = 0.975 leading to a 5% increase in induced power. When the tip loss factor is introduced the induced power correcting factor will thus be 1.10.

For twisted blades with the typical negative twist of 8° from root to tip, as in the reports available for analysis, which approach the ideal more closely, the correcting factors are taken as 1.10 without the tip loss factor, or 1.05 when tip losses are separately accounted for.

The 5% tip loss is confirmed by flight tests reported in Ref. 10.

The above corrections for rotational and tip losses have been found to be quite adequate for back analysis from flight tests, but if more refined estimates are required in performance calculations methods of estimation for rotors of specific operating characteristics are given by Talkin in Ref. 1.

If it is desired to take account of the actual planform and pitch distribution of a particular rotor the induced power loss can be estimated in the following way.

From simple blade element theory, with the usual assumptions, the thrust of a blade element of chord c at radius r is:

$$\Delta T = b \cdot \frac{\rho}{2} \cdot (\Omega r)^2 a (\theta_r - \phi_r) c \cdot dr \quad \dots(5)$$

where $\theta_r - \phi_r$ is the section angle of attack, ϕ_r being $\frac{u}{\Omega r}$ where u is the total flow velocity at the element.

$u = V_c + v_r$ where v_r is the induced velocity and V_c is the vertical climb velocity.

From momentum theory the thrust produced by an annular ring of width dr at radius r is

$$\Delta T = 4\pi\rho u v_r \cdot r \cdot dr. \quad \dots(6)$$

Equating (5) and (6) gives:

$$v_r = \left(\frac{V_c}{2} + \frac{bca\Omega}{16\pi} \right) \left(-1 + \sqrt{1 + \frac{2\Omega r \left(\theta_r - \frac{V_c}{\Omega r} \right)}{4\pi V_c^2 + \frac{bca\Omega}{16\pi} + V_c + \frac{bca\Omega}{16\pi}}} \right) \quad \dots(7)$$

Introducing/

Introducing the local solidity $\sigma_x = \frac{bc}{\pi R}$ based on the blade chord at radius r , and writing $x = r/R$ we get:

$$v_x = \left(\frac{V_c}{2} + \frac{\sigma_x \cdot a \cdot \Omega R}{16} \right) \left(-1 + \sqrt{1 + \frac{2(\theta_x x \Omega R - V_c)}{\frac{4V_c^2}{\sigma_x \cdot a \cdot \Omega R} + V_c + \frac{\sigma_x \cdot a \cdot \Omega R}{16}}} \right) \dots (8)$$

Expression (8) is completely general and gives the induced velocity at any blade element at radial distance x and having any chord and pitch angle θ .

Montgomery Knight in Ref. 11 has given the same expression derived by application of the vortex theory. Having obtained the induced velocity the inflow angle ϕ at any blade element is given by:

$$\phi_x = \frac{v_x + V_c}{\Omega r} \dots (9)$$

So the general expression for the inflow angle is:

$$\phi_x = \left(\frac{V_c}{2x\Omega R} + \frac{\sigma_x \cdot a}{16x} \right) \left(-1 + \sqrt{1 + \frac{2(\theta_x x \Omega R - V_c)}{\frac{4V_c^2}{\sigma_x \cdot a \cdot \Omega R} + V_c + \frac{\sigma_x \cdot a \cdot \Omega R}{16}}} \right) + \frac{V_c}{x\Omega R} \dots (10)$$

In the hovering case where $V_c = 0$ the expressions simplify to:

$$v_x = \frac{\sigma_x \cdot a \cdot \Omega R}{16} \left(-1 + \sqrt{1 + \frac{32 \theta_x \cdot x}{\sigma_x \cdot a}} \right) \dots (11)$$

$$\phi_x = \frac{\sigma_x \cdot a}{16 \cdot x} \left(-1 + \sqrt{1 + \frac{32 \theta_x \cdot x}{\sigma_x \cdot a}} \right) \dots (12)$$

and of course the blade angle of attack is:

$$\alpha_x = \theta_x - \phi_x \dots (13)$$

An alternative form of (11) which is more convenient for tabular computation is:

$$v_x = \Omega R \left[\frac{-2\sigma_x}{16} + \sqrt{\left(\frac{2\sigma_x}{16} \right)^2 + \frac{2\sigma_x \theta_x \cdot x}{8}} \right] \dots (14)$$

Estimates made in the above way at a number of radial stations (say at intervals of 0.1 from $x = 0.1$ to $x = 1.0$) will give the thrust and induced power for any rotor since:

$$\text{Thrust} = T = 4\rho\pi R^2 \int v_x^2 \cdot x \cdot dx \quad \dots(15)$$

$$\text{Induced Horsepower} = HP_i = \frac{4\rho\pi R^2}{550} \int v_x^3 \cdot x \cdot dx \quad \dots(16)$$

The integrations are performed graphically by plotting $v_x^2 \cdot x$ and $v_x^3 \cdot x$ against radial distance x and multiplying the area under the curves by $4\rho\pi R^2$ and $\frac{4\rho\pi R^2}{550}$ respectively.

If the thrust and induced power estimates are required in terms of the usual non-dimensional thrust and torque coefficients we can write

$$\frac{d C_T}{dx} = \sigma_x \cdot \frac{a}{2} \cdot a_x \cdot x^2 \quad \dots(17)$$

$$\frac{d C_{Q_i}}{dx} = \sigma_x \cdot \frac{a}{2} \cdot \phi_x \cdot a_x \cdot x^3 \quad \dots(18)$$

Plotting dC_T/dx and dC_{Q_i}/dx against radial distance x and taking the area under the curves gives C_T and C_{Q_i} directly.

2.3 Blade Profile Drag and Profile Drag Power

2.31 If information is available as to the drag/angle of attack characteristics of the blade sections in two-dimensional flow, corrected for compressibility and Reynold's number, the profile drag torque coefficient can be obtained since, corresponding to expression (18), we can write:

$$\frac{dC_{Q_p}}{dx} = \frac{\sigma_x}{2} \cdot C_D \cdot x^3 \quad \dots(19)$$

As before $\frac{d C_{Q_p}}{dx}$ is plotted against x and the area under the curve gives the rotor profile torque coefficient C_{Q_p} . The rotor torque coefficient is of course the sum of the induced and profile drag torque coefficients.

2.32 The methods of obtaining rotor power based on equations (16), (18) and (19) are useful when comparing measured performance with theory, but as indicated require a knowledge of the drag/angle of attack characteristic of the blade sections.

For routine estimates however it is suggested that it is more appropriate to relate the mean drag coefficient of the blades to their mean lift coefficient, since no estimate of the aerofoil lift slope is required and the mean lift coefficient when hovering is very simply determined as

$$\overline{C_L} = \frac{6.6 \cdot C_T}{\sigma} \quad \dots(20)$$

The analyses presented later in this report will be given in this form.

The angle of attack at the representative blade section where the lift coefficient is $\overline{C_L}$ will be $\frac{6.6 C_T}{\sigma a}$. Where the lift slope is required in the following analyses, it will be taken as 5.60 per radian, which value was derived from some of the flight tests where the accuracy of blade pitch angle measurement was known to be satisfactory.

2.33 In analyzing test results to derive the mean blade drag coefficient, the method to be adopted will depend on the way in which the test data is presented.

Where the hovering test data is presented in terms of C_T and C_Q we have the following expression connecting the two coefficients.

$$C_Q = K \cdot \frac{C_T}{2} \sqrt{\frac{2 C_T}{B^2} + \frac{\sigma \delta}{8}} \quad \dots(21)$$

Equation (21) is the same as (10) of Ref. 12 but with the tip loss factor B included. δ is the mean blade drag coefficient and K the correcting factor for non-uniform induced velocity, i.e., 1.1 for untwisted blades or 1.05 for conventional blades with some 8° negative twist.

When the mean drag coefficient is related to section angle of attack it is usually referred to the angle of attack of the blade section at 0.75R, but this is incorrect.

The usual expression used for the hovering torque coefficient in the rotor theory as developed by Glauert¹³ and Lock¹⁴ (see also (6) of Ref. 12) for untwisted blades and without tip loss factor is:

$$C_T = \frac{\sigma a}{4} \left(\frac{2}{3} \theta_{.1} - \lambda \right) \quad \dots(22)$$

or
$$\frac{6 C_T}{\sigma a} = \theta_m - \frac{3}{2} \lambda \quad \dots(23)$$

Now $\frac{6 C_T}{\sigma a}$ is simply the mean blade angle of attack and $\frac{3}{2} \lambda$ is ϕ , the inflow angle at 2/3R, so that it is the angle of attack at this radius to which the mean lift coefficient and therefore the mean drag coefficient is to be related.

The simple Glauert/Lock theory was extended by Wheatley¹⁵ to cover twisted blades and to include the tip loss factor, and the Wheatley theory has been simplified by Bailey¹⁶ who gives the thrust coefficient relationship in the form:

$$\frac{2 C_T}{\sigma a} = t_1 \lambda + t_2 \theta_0 + t_3 \theta_1 \quad \dots(24)$$

N.B. In comparing (24) with (23) note should be taken of the change in sign convention, λ in (24) being negative in helicopter powered flight. Equation (23) refers only to the hovering case but (24) is quite general and the values of the coefficients t_1 , t_2 and t_3 are tabulated over a range of the tip speed ratio μ . For convenience, these coefficients extended down to the hovering case ($\mu = 0$) are plotted in Fig. 1.

In the hovering case the ratio of the coefficients t_2 to t_1 is 0.645 and this is the radius of the representative blade section having the angle of attack to which the mean lift and drag coefficients are related.

It may be noted here that the mean blade lift coefficient under any condition of flight is given by $\frac{2 C_T}{\sigma t_2}$.

The correct interpretation of the common statement that the blade section at 0.75R is representative is shown by the fact that the ratio of the Bailey coefficients of θ_1 and θ_0 in his thrust and torque equations is close to 0.75 over the normal range of μ values, indicating that rotors with twisted or untwisted blades will have the same characteristics if the blade angles at 0.75R are the same.

The Bailey expressions have been further extended by Lichten¹⁷ to cover non-uniformity of induced velocity from front to rear of the disc, and also to cover taper, and the modified coefficients are given in the paper.

There are a few vertical climb tests available in the reports which are analysed and in these cases the equation for torque coefficient corresponding to (21) becomes:

$$C_Q = K \cdot \frac{C_T}{2} \sqrt{\frac{2 C_T}{B^2} + \left(\frac{V_c}{\Omega R}\right)^2} + \frac{1}{2} \cdot \frac{V_c}{\Omega R} \cdot \frac{C_T}{B^2} + \frac{\sigma \delta}{8} \quad \dots(25)$$

where V_c is the vertical rate of climb in ft/sec.

When the test data is given directly in horse power at the rotor the induced power hovering is given by:

$$HP_i = K \times 0.0264 \times W \times \sqrt{W} \times \sqrt{\frac{P_0}{\rho}} \quad \dots(26)$$

Here K is 1.15 for rectangular untwisted blades and 1.10 for blades having about 3° negative twist.

The difference between the total power at the rotor and the induced power is the blade profile drag power HP_p and the mean blade drag coefficient is given by:

$$HP_p = \frac{\rho \sigma \delta \pi R^2 (\Omega R)^3}{4400} \quad \dots(27)$$

It/

It should be noted that in vertical climb the induced velocity is less than when hovering, since the rotor is handling a greater mass of air which requires to be accelerated less to produce the same thrust.

The induced velocity v_c in vertical climb is given by:

$$v_c = \frac{-V_c + \sqrt{V_c^2 + 4 v_h^2}}{2} \quad \dots(28)$$

where V_c is the rate of vertical climb in ft/sec., and v_h the induced velocity when hovering, which is, of course, when tip losses are ignored:

$$v_h = K \cdot \sqrt{\frac{W}{2\rho}} = K \cdot \Omega R \sqrt{\frac{C_T}{2}} \quad \dots(29)$$

In deriving HP_p for use in (27) from vertical climb tests the equation for induced power corresponding to (26) is:

$$HP_i = K \cdot \frac{v_c}{550} \cdot \sqrt{\frac{P_0}{\rho}} \cdot W \quad \dots(30)$$

2.4 Forward Flight

In forward flight both the induced and profile drag power are modified, and when analyzing tests giving measured rotor power it is convenient to relate these powers to the corresponding power in the hovering condition at the same tip speed, density and operating C_T .

2.4.1 Induced Power in Forward Flight

In forward flight on the usual assumptions the induced velocity is given by:

$$v = \frac{T}{2\pi R^2 \rho V} \quad \dots(31)$$

and hence the induced power in ft/lb/sec units as:

$$P_i = \frac{T^2}{2\pi R^2 \rho V} \quad \dots(32)$$

Expression (32) by analogy with lifting aerofoil theory is correct for elliptic loading, so for the practical rotor we shall use

$$P_i = \frac{1.1 T^2}{2\pi R^2 \rho V} = \frac{1.1 Wv}{2\rho V} \quad \dots(33)$$

Since/

Since the induced hovering power is $1.15 W \sqrt{\frac{W}{2\rho}}$, the ratio of the induced power in forward flight to that in hovering at the same density, which we shall use as a correcting factor is:

$$(f)_i = \frac{13.85 \sqrt{W}}{V} \quad \dots(34)$$

As explained in the Appendix this is correct only above about 60 ft/sec forward speed. Correct low speed values of $(f)_i$ are given in Fig. 13.

The expression for induced power corresponding to (26) is:-

$$HP_i = K \times 0.0264 \times W \times \sqrt{W} \times \sqrt{\frac{\rho_0}{\rho}} \times (f)_i \quad \dots(35)$$

In many of the American reports the test results are given in the form of (D/L) ratios as first suggested by Wheatley¹⁵ and later extended by Bailey and Gustafson⁴ who wrote all the power components of a helicopter as (D/L) ratios and equated their sum to a ratio P/L, where P is the drag equivalent, at the speed in question, of the total power absorbed so that:

$$\text{Horsepower} = HP = \frac{\left(\frac{P}{L}\right) \times W \times V}{550} \quad \dots(36)$$

$$\frac{P}{L} = \left(\frac{D}{L}\right)_p + \left(\frac{D}{L}\right)_i + \left(\frac{D}{L}\right)_t + \left(\frac{D}{L}\right)_c + \left(\frac{D}{L}\right)_f$$

rotor profile rotor induced tail rotor climb parasite drag

Bailey¹⁶ has shown that the rotor induced drag/lift ratio can be written

$$\left(\frac{D}{L}\right)_i = \frac{C_T}{2 \mu (\lambda^2 + \mu^2)^{\frac{1}{2}}} \quad \dots(37)$$

which at values of μ greater than 0.15 can, without loss of accuracy, be written as:

$$\left(\frac{D}{L}\right)_i = \frac{C_T}{2 \mu^2} = \frac{C_L}{4} \quad \dots(38)$$

Where C_L is the lift coefficient referred to the disc area, i.e.,

$$C_L = \frac{W}{\pi R^2 \frac{\rho}{2} V^2} \quad \dots(39)$$

The Bailey expressions, however, are based on uniform induced velocity, though with tip corrections, so in the analyses of the present paper the expression is used in the form:

$$\left(\frac{D}{L} \right)_i = K \cdot \frac{C_T}{2 \mu^2} = K \cdot \frac{C_L}{4} \quad \dots(4.0)$$

Where $K = 1.1$ for untwisted blades and 1.05 for blades with 8° negative twist.

2.42 Blade Profile Drag and Profile Drag Power

2.421 The blade profile drag power in forward flight is simply the power for hovering under the same operating conditions multiplied by $(1 + 4.65 \mu^2)$ so that in the general form (27) becomes:

$$HP_p = \frac{\rho \sigma \delta \pi R^2 (\Omega R)^3}{44.00} (1 + 4.65 \mu^2) \quad \dots(4.1)$$

where δ is the mean effective blade profile drag coefficient. The profile drag power is of course obtained as before as the difference between the total measured rotor power and the induced power, as estimated by the methods of paragraph 2.41. If obtained from the tests directly in horse power (41) gives the mean drag coefficient as:

$$\delta = \frac{HP_p \times 44.00}{\rho \sigma \pi R^2 (\Omega R)^3 (1 + 4.65 \mu^2)} \quad \dots(4.2)$$

Where the test data is presented in the form of drag/lift ratios the expression is:

$$\delta = \frac{\left(\frac{D}{L} \right)_P \times C_T \times \mu \times \delta}{\sigma (1 + 4.65 \mu^2)} \quad \dots(4.3)$$

2.422 The mean effective drag coefficient in forward flight is related to the mean drag coefficient in hovering, and for routine performance calculations it is suggested that the blade drag/lift coefficient relationship derived from hovering tests should be treated as giving the "basic" blade drag, and that the "effective" drag at forward speed should be obtained by applying appropriate correcting factors.

We then have

$$\delta_{\text{forward speed}} = \delta_{\text{hovering}} \times (f)_\mu \times (f)_s \times (f)_c \quad \dots(4.4)$$

$(f)_\mu$ is a correcting factor depending on the lift distribution across the rotor disc and is a function of the tip speed ratio. $(f)_s$ is a factor giving the increase in effective drag when blade tip stalling occurs, and $(f)_c$ is a compressibility factor. These three factors will be derived in the analysis of the N.A.C.A. tests in paragraph 3.

2.43 Retreating Blade Tip Angle of Attack

Before the $(f)_s$ stalling factor can be determined it is necessary to know the retreating tip angle of attack. The following gives methods for making estimates.

If θ_m is the blade pitch angle of an untwisted blade and a_1 is the flapping angle, the maximum blade angle of attack will be

$$\theta_{max} = \theta_m + \alpha_1 + \phi_t$$

where ϕ_t is the inflow angle at the tip = $\frac{v}{\Omega R} = \lambda$. Simple theory (see for example equations (1) and (3) of Ref. 12) gives θ_m and a_1 in the form:

$$\theta_m = \frac{\frac{6 C_T}{\sigma a} \left(1 + \frac{3}{2} \mu^2\right) - \frac{3}{2} \lambda \left(1 - \frac{1}{2} \mu^2\right)}{1 - \mu^2 + \frac{9}{4} \mu^4} \dots(45)$$

$$a_1 = \frac{\frac{8\mu}{3} \left(\theta_m + \frac{3}{4} \lambda\right)}{1 + \frac{3}{2} \mu^2} \dots(46)$$

Putting θ_m from (45) in (46) and expanding we get the maximum tip angle of attack in the form:

$$\theta_{max} = \frac{\left[\begin{matrix} 3 & 8 \\ 1 + \frac{3}{2} \mu^2 + \frac{3}{2} \mu & 3 \end{matrix} \right] \left[\frac{6C_T}{\sigma a} \left(1 + \frac{3}{2} \mu^2\right) - \frac{3}{2} \lambda \left(1 - \frac{1}{2} \mu^2\right) \right] + 2\lambda \mu \left(1 - \mu^2 + \frac{9}{4} \mu^4\right)}{\left(1 - \mu^2 + \frac{9}{4} \mu^4\right) \left(1 + \frac{3}{2} \mu^2\right)} + \lambda \dots(47)$$

For convenience in calculation the standard terms in the above expression are plotted in Fig. 2.

An expression, which so far as is known has never been derived before can also be obtained for twisted blades. The analysis, which is too lengthy to be given here, for linear twist of θ_1 radians results in the addition of a new term in (47). This term is:

$$\text{Change in } \theta_{max} \text{ for } \theta_1 \text{ twist} = \theta_1 \cdot \frac{\left(\begin{matrix} 3 & 8 \\ 1 + \frac{3}{2} \mu^2 + \frac{3}{2} \mu & 3 \end{matrix} \right) \left(\frac{1}{2} \frac{1 + \frac{9}{4} \mu^2 + \frac{9}{4} \mu^4}{4} \right) - \frac{2}{3} \mu \left(1 - \mu^2 + \frac{9}{4} \mu^4\right)}{\left(1 - \mu^2 + \frac{9}{4} \mu^4\right) \left(1 + \frac{3}{2} \mu^2\right)} \dots(48)$$

That is to say that linear negative twist reduces the maximum tip angle of attack by the factor of θ_1 in (48) and this reduction is independent of the rotor parameters or operating condition except the tip speed ratio μ .

The values of the change factor are plotted in Fig. 3.

In practice the calculation for twisted blades is made by (47) and the tip angle so determined is reduced by the angle given by (48).

In order to use (47) and (48) it is necessary to know the value of λ .

In level flight the incidence of the rotor disc is given by:

$$\tan \alpha = - \left(\frac{H}{W} + \frac{D}{W} \right) \quad \dots(49)$$

where H is the rotor force in the plane of the disc.

In terms of the rotor parameters and operating conditions (49) can be rewritten

$$\tan \alpha = - \left(\frac{\delta \rho V \Omega R}{4 \sigma} + \left(\frac{D}{L_f} \right) \right) \quad \dots(50)$$

where $\left(\frac{D}{L_f} \right)$ is the parasite drag/lift ratio of the helicopter at speed V .

The value of λ is then obtained from the alternative expression for $\tan \alpha$ (equation (4) of Ref. 12) which for small values of α reduces to:

$$\tan \alpha = \frac{\lambda}{\mu} + \frac{C_T}{2 P^2 \mu^2} \quad \dots(51)$$

Alternatively we may write

$$\lambda = - \left(\frac{V \sin \alpha + v}{\Omega R} \right) \quad \dots(52)$$

where
$$v = \frac{1.1 w}{2 \rho V} ,$$

From time to time various writers have suggested simple semi-empiric formulae to give an approximate indication of the limiting speed at which tip stalling will become excessive. These are commonly of the form

$$V_{\text{limiting}} = 0.75 \Omega R - K \sqrt{\frac{w}{\sigma}} \quad \dots(53)$$

Such/

Such formulae are not satisfactory since they take no account of the parasite drag/lift ratio which largely influences the disc angle of attack and therefore λ , and the value of K relates to an arbitrary maximum tip angle of attack.

A similar form of expression can however be made quite general by introducing the parasite drag/lift ratio and relating K directly to the maximum tip angle of attack. In this form K can be written as:

$$K = \frac{\left[0.75 - \left\{ 0.8 + 4 \left(\frac{D}{L} \right)_f \right\} \mu \right] \times \sqrt{\frac{P}{\rho_0}} \times \Omega R}{\sqrt{\frac{w}{\sigma}}} \quad \dots(54)$$

or

$$K = \frac{\left[0.75 - \left\{ 0.8 + 4 \left(\frac{D}{L} \right)_f \right\} \mu \right]}{0.0488 \sqrt{\frac{C_T}{\sigma}}} \quad \dots(55)$$

The value of K computed by (54) or (55) is related to the maximum tip angle of attack in Fig. 3 which gives the tip angle directly, for untwisted blades. For twisted blades the tip angle so computed is reduced by the angle given by (48), the factor of θ_1 being given in the inset curve of Fig. 3.

2.44 Blade Flapping Angle and Control to Trim in Forward Flight

All the early rotating wing theories (e.g., Ref. 14 and 15) referred to the autogiro in which control was achieved by tilting the rotor hub, i.e., to a pure flapping system, in which there is no feathering with respect to the shaft, but in which there is acquired feathering in the disc plane in forward flight due to the rotor disc (tip-path plane) tilting backwards with respect to the shaft. Lock¹⁴ showed the equivalence of feathering and flapping, but there has always been considerable confusion since the various formulae, which will be found in the literature, differ in form according to the axes of reference.

Most of the confusion was removed by Stewart¹⁸ but some difficulty may still be experienced when applying the theory to the modern helicopter, which in the commonest form involves both flapping and feathering, the attitude of the rotor disc resulting from a combination of shaft tilt, applied feathering (control) relative to the shaft and flapping, as shown in Fig. 3 of Ref. 18. The control feathering is achieved by a swashplate, or mechanical equivalent, rotating with the blades and linked to them so that a tilt of the plate produces cyclic feathering. Any remaining confusion should be removed when once it is appreciated that when the rotor is revolving the blades do not change pitch as referred to the plane of the swashplate however the latter may be tilted. The axis of the swashplate (axis of no-feathering) is thus equivalent to the shaft axis of a pure flapping system. To clarify, Figs. 2(a) and 3 of Ref. 18 are redrawn in modified form in Fig. 4 of this report.

In the figures the rotor disc altitude to the flight path is the same, since the flight conditions are assumed to be the same so that the longitudinal flapping amplitude a_1 of Fig. 4a (i.e., the backward tilt of the rotor disc with respect to the shaft) is the same as a_1 of Fig. 4(b) the angle between the disc and the swashplate axis (axis of the feathering) and is therefore given by equation (23) of Ref. 18, i.e., with the sign convention of the present report:

$a_1/$

$$a_1 = 2 \mu \cdot \frac{\frac{4}{3} \theta_{in} + \lambda}{1 + \frac{3}{2} \mu^2} \quad \dots(56)$$

where λ is the inflow ratio referred to the rotor disc axis.

Alternatively, and what is identical,

$$a_1 = 2 \mu \cdot \frac{\frac{4}{3} \theta_{in} + \lambda_{nf}}{1 - \frac{1}{2} \mu^2} \quad \dots(57)$$

where λ_{nf} is the inflow ratio referred to the no-feathering axis.

From Fig. 4(b) we have the disc angle of attack to the flight path

$$\alpha = \alpha_s + a_{1s} = \alpha_s + (B_{1s} - a_1) \quad \dots(58)$$

where a_{1s} is the flapping amplitude with respect to the shaft and B_{1s} is the applied feathering control to trim.

We have also from (49), made general by including τ the angle of the flight path to the horizontal,

$$\tan(\alpha - \tau) = -\left(\frac{H}{W} + \frac{D}{W}\right)$$

and from (37) of Ref. 18

$$B_{1s} - a_1 = \frac{H}{W} - \frac{f}{h} + \frac{M_f}{Wh} \quad \dots(59)$$

and finally from (51) of Ref. 18

$$\alpha_s = \tau + \frac{D}{W} \cos \tau + \frac{H}{W} - (B_{1s} - a_1) \quad \dots(60)$$

where τ is the flight path angle to the horizontal.

To use the alternative expression for flapping amplitude of (57) it is necessary to estimate λ_{nf} . Nikolsky and Seckel have given an expression for this in a little known report (Ref. 19). The expression is:

$$t_1 \lambda_{nf}^2 + \frac{2 C_T}{\sigma a} t_2 \lambda_{nf} + \left(\frac{2 C_T}{\sigma a} \right)^2 t_7 + t_{22} \cdot \frac{\delta}{a} + \frac{2 C_Q}{\sigma a} = 0 \quad \dots(61)$$

The values of the coefficients in this expression are given in Table I.

Table I

Coefficients in Nikolsky and Seckel Expression for λ_{nf}

μ	t_1	t_2	t_7	t_{22}
0.20	-0.01	0.935	0.38	-0.260
0.25	-0.015	0.895	0.59	-0.265
0.30	-0.021	0.847	0.825	-0.272
0.35	-0.0285	0.795	1.09	-0.280
0.40	-0.037	0.74	1.38	-0.289
0.45	-0.0475	0.67	1.70	-0.299
0.50	-0.06	0.60	2.02	-0.310

When λ_{nf} is obtained directly by (61) the "incidence" of the no-feathering axis α_{nf} is given by an expression in the same form as (51), which still holds good with the new axis of reference, i.e.,

$$\tan \alpha_{nf} = \frac{\lambda_{nf}}{\mu} + \frac{C_T}{2 B^2 \mu^2} \quad \dots(62)$$

B_{1S} , the applied feathering for control and trim, is then given by:

$$\alpha_{nf} = \alpha_S + B_{1S} \quad \dots(63)$$

3. Analysis of American Reports

3.1 Hovering

3.11 NACA Technical Note No. 626¹¹

This report is of no great value in respect of the main purpose of the present report, but is of interest as being one of the earliest static analyses of the lifting rotor and as developing equation (8) for induced velocity from vortex theory. Four model rotors of 5' diameter were tested and the experimental thrust and torque coefficients compared with theoretical estimates made by the use of expressions of the same form as (17), (18) and (19). The estimated thrust coefficients were consistently higher than the experimental values, while the experimental torque coefficients departed more and more from estimates as the blade angles and torque coefficients increased. The profile drag torque was obtained using an expression of the form $C_D = C_{D_{min}} + c\alpha^2$ for the blade drag coefficients, using a value for e based on tunnel tests. This value had to be increased by a factor 1.67 to bring estimates into agreement with experimental values.

The same equations have been used to estimate thrust and torque coefficients for the rotors of Refs. 20 and 21 but using the profile drag torque obtained from the mean blade drag coefficients derived in para. 3.14 of this report. For the untwisted YR-4B blades of Ref. 20 the method gave thrust coefficients about 7% higher than measured and about 4% higher torque coefficients when the integration was carried out to the tip. This discrepancy can be attributed to tip losses and when the integration was carried only to 0.97R the agreement became almost perfect. This is confirmed by the tests on the same rotor in Ref. 10. The agreement is not so good in the case of the twisted blades of Ref. 21, where the thrust was overestimated by about 2% and the induced torque by 3%. This can be explained by slight twisting of the blades reducing the nominal blade pitch angles in flight.

3.12 Full Scale Tunnel Tests on Two 25' Diameter Rotors

Refs. 22 and 23 give static thrust and torque coefficients for two rotors both of constant chord without twist and both fabric covered over a plywood nose. One rotor was of 0012.6 aerofoil section with fairly good finish, but on the second where the aerofoil was 23012.6 the aerofoil contour was not true.

The tests have been analyzed to give the "basic" (i.e. hovering) mean blade drag coefficients as a function of mean blade lift coefficient following the method of para. 2.33 and the results are given in Fig. 5. The difference in mean blade drag characteristics between the two aerofoils is very small though the 23012.6 section becomes somewhat better at high lift coefficients. The comparison is however **impaired** by the differences in surface finish, the 23012.6 being the worse of the two. All we can really say is that the tests are consistent with the available tests of other fabric covered rotors, and that no difference due to difference in blade aerofoil section is indicated.

3.13 Full Scale Tunnel Tests on Six Rotors

In Ref. 24 the results of static tests on six sets of blades for the helicopter of Refs. 20 and 21 are given.

These blades for which the mean drag/mean lift coefficient relationships are given in Fig. 6 are identified below.

- A. The production blades of Ref. 20. Radius 19', aerofoil NACA 0012, untwisted, solidity 0.06. They are fabric covered with 6" rib spacing.
- B. As blades A but with accurately formed leading edge and closer rib spacing to maintain better aerofoil contour.
- C. As B but with negative twist of 8° from root to tip.

- D. Construction as B but only 18' radius and solidity 0.061 and with 11.9° negative twist.
- E. Plywood covered blades, Radius 19', aerofoil NACA 23015 reflexed, untwisted, solidity 0.042. These blades are substantially the same as those flight tested in Ref. 33 except for a balancing tab near the tip.
- F. As E but with negative twist of 8° from root to tip, and substantially the same as those flight tested in Ref. 21.

The mean blade drag/mean blade lift coefficient relationships from the measured thrust and torque coefficients are given in Fig. 6. Unfortunately the absolute values given by these tests are questionable, but the authors believe the comparative results to be reliable. For what they are worth the tests result in the comparative figures given in Table 2 for the six rotors fitted to the test helicopter of Refs. 20 and 21. There are flight test hovering figures available for rotors A and F and these figures and estimates using the methods of paras. 2.2 and 2.3 and the suggested drag coefficient curves of Fig. 7 are included.

The extent to which the tunnel measurements are below the absolute figures is indicated by the above comparison though there are some anomalies, as for instance the higher power required by F than E at high r.p.m., and the surprising apparent improvement in B over A.

The test figures do however indicate that blade surface condition has an important effect on performance and that the best from a given rotor design can only be obtained if the blades are well finished and have a surface which will maintain accurate contour in flight. They also show the improvement, within the operating range covered, obtainable by working at lower rotor speeds.

3.14 Flight Tests

Refs. 20 and 21 gave the results of full scale flight tests on the YR-4B helicopter equipped with the production blades and an alternative set with plywood cover, but of lower solidity and with 8° negative twist. These two sets of blades correspond to the A and F blades of para. 3.13. Unfortunately there are only two tests for the fabric covered blades, but in association with some of the other tests discussed they do serve to establish the relative drag characteristics of representative fabric and plywood covered blades.

All hovering tests available have been plotted together. From them it is not possible to trace any difference due to different blade aerofoil sections which differences are so small as to be masked by differences in surface finish.

The two mean drag curves resulting are given in Fig. 7.

These two curves are considered to be representative of fabric covered and good plywood covered blades generally, and to be adequate for performance estimates for conventional blades.

In the theoretical treatments on which the NACA methods of performance estimates are based (vide for example Refs. 4 and 16) the aerofoil characteristics are closely represented by a power series, the one used as representative of good blades being:

$$c_{d_0} = 0.0087 - 0.0216 \alpha_0 + 0.400 \alpha_0^2. \quad \dots(64)$$

Table II

Comparative Rotor Power Required to Hover at Sea Level
Six Rotors from Tests in NACA ARR.No.L5F25b
Assumed Gross Weight of Helicopter 2500 lb

Rotor	Engine Speed r.p.m.						Gross Weight to Hover for 140.0 h.p. From Tests
	2300			2100			
	$C_T = 0.00387$			$C_T = 0.00464$			
	Horse Power to Hover Tunnel Test	Horse Power to Hover Estimate	Gross Weight to Hover For 147.7 h p. from Tests	Horse Power to Hover Tunnel Test	Horse Power to Hover Flight Test	Horse Power to Hover Estimate	
A	147.7	160.5	2500 lb	140.0	154.0	151.1	2500 lb
B	131.1	156.5	2733 lb	126.9		147.5	2682 lb
C	137.4	157.5	2655 lb	130.8		143.5	2628 lb
D	140.8	152.5	2597 lb	134.8		144.5	2574 lb
E	127.6	143.7	2778 lb	124.7		139.0	2715 lb
F	128.2	139.2	2798 lb	123.4	135.0	134.5	2758 lb

1
12
1

This/

This corresponds to the NACA 23012 aerofoil at the appropriate Reynolds number with the c_{d_0} minimum increased by a roughness factor of 17%. The drag/lift curve from (64) is plotted for comparison with the mean curve from flight tests in Fig. 7.

The curves of Fig. 7 will not hold of course for unconventional aerofoil sections such as the low drag aerofoils, e.g., Ref. 37 which have at times been suggested for helicopter blades. In such a case the actual aerofoil data will have to be used and to permit analytical methods this will have to be represented by a power series, i.e.,

$$c_{d_0} = \delta_0 - \delta_1 \alpha_0 + \delta_2 \alpha_0^2 \dots (65)$$

The values of δ_0 , δ_1 and δ_2 can be derived by the method explained in Ref. 16.

When this procedure is necessary the general torque equation for vertical climb corresponding to (25) becomes:

$$C_Q = K \cdot \frac{C_T}{2} \sqrt{\frac{2 C_T}{B^2} + \left(\frac{V}{\Omega R}\right)^2} + \frac{1}{2} \cdot \frac{V}{\Omega R} \cdot \frac{C_T}{B^2} + \frac{\sigma \delta_0}{8} + \frac{2}{3} \cdot \frac{\delta_1}{a} \cdot \frac{C_T}{B^2} + \frac{4 \delta_2}{\sigma a^2} \left(\frac{C_T}{B^2}\right)^2 \dots (66)$$

3.15 Full Scale Tunnel Tests on Contra-rotating Coaxial Rotors

Ref. 25 gives the results of full scale tunnel tests on a pair of coaxial rotors made to determine the static thrust performance. The two rotors were each two bladed, 25 feet in diameter mounted coaxially 9.5% of the rotor diameter apart. The rotors had plywood covers and were tapered both in plan form and in thickness, but were untwisted. The aerofoil sections were of the NACA four digit symmetrical type and of solidity 0.027 each (i.e., 0.054 for the combination). There was an appreciable difference in performance between tip speeds of 327 feet per second and 450 feet per second which were attributable to scale effect. The difference however became small at tip speeds of 450 and 500 feet per second.

The tests cover a range of thrust coefficient from $C_T = 0$ to $C_T = 0.00557$ for the coaxial arrangement and to $C_T = 0.00346$ for the single rotor at a tip speed of 500 feet per second.

Within the experimental accuracy the profile torque coefficient at $C_T = 0$ for the coaxial arrangement was twice that for either of the rotors separately. The mean drag coefficients derived for the single and coaxial tests when plotted against mean blade lift coefficient also fall on a single curve.

The tests confirm that two rotors mounted coaxially behave as one rotor having the combined solidity of the two.

3.16 Some Theoretical Investigations

3.161 Effect of Rotor Tip Speed on Hovering Performance

Ref. 26 gives a theoretical investigation into the effect of tip speed on hovering performance using the general performance equation for vertical climb (16) and calculating C_T by methods analogous to those given in para. 2.2 using the profile drag equation (64).

The comparative thrust, rotor shaft power and rate of vertical climb for a typical helicopter of solidity 0.06, and parasite drag 178 lb at 100 feet per second are given in the following table.

Table III

Vertical Flight Performance of a Typical Helicopter
Weight 2700 lb, Diameter 41 feet, Solidity 0.06, 8° Negative Twist

Tip Speed ft/sec	Hovering Power at 2700 lb	Hovering Thrust for 200 h.p.	Rate of Vertical Climb 2700 lb 200 h.p.
300	131	3640 lb	1300 ft/min
340	133	3607 "	1237 "
380	137	3590 "	1184 "
420	144	3500 "	1085 "
460	150	3430 "	970 "
500	160	3320 "	800 "
540	170	3170 "	600 "
580	183.5	2980 "	370 "
620	200	2700 "	-

The helicopter considered in this analysis corresponds to a cleaned up version of the YR-4B of Ref. 20 the tip speed corresponding to maximum power being 500 ft/sec. The tip speed for such a type could be limited by power available rather than by blade tip stalling and no appreciable loss in speed would be involved by operating at 440 ft/sec. As the table shows, lowering the hovering tip speed from 500 to 440 ft/sec would decrease the hovering power required at fixed weight by 8%, increase the thrust available at fixed power by 5% and increase the rate of vertical climb by about 28%.

3.162 Effect of Blade Profile Drag Characteristics on Hovering Performance

Ref. 27 gives theoretical estimates of hovering thrust for a typical helicopter with three sets of blades, one representative of "rough conventional" blades corresponding to the fabric covered blades of the YR-4B of Ref. 20, one with smooth NACA 23015 section and the other with the NACA J.H.13.5, one of the low drag sections of Ref. 37. For comparison the thrusts on the assumption of zero profile drag and uniform induced velocity with zero profile drag are included.

The assumed rotor characteristics are:

Rotor diameter	40 ft
Solidity	0.07
Blade plan-form	Rectangular
Blade twist	None
Power available at rotor	260 h.p.

The calculations show that a change from the rough conventional section to smooth 23015 section at a typical tip speed of 500 ft/sec results in an increase in hovering thrust of 350 lb (9.6%). Changing from the 23015 section to the smooth low drag J.H.13.5 results in a further increase of 200 lb. It is worthy of note that only about 300 lb more could be gained if the profile drag could be made zero, with a further 300 lb with ideal twist giving uniform induced velocity.

3.163 Effect of Blade Twist, and Plan-form Taper on Hovering Performance

Ref. 28 gives a theoretical analysis of the hovering performance of rotors with various combinations of twist and plan-form taper. The analysis followed the lines of equations (11), (12) and (13), and equations (17), (18) and (19) were integrated graphically to give curves of C_T against C_Q for each of the combinations.

The blade section drag characteristics were as represented by the power series (64).

Estimates are also given for the ideally twisted blade, i.e., a blade so twisted as to produce uniform inflow and consequently minimum induced losses when rotational losses are ignored. Tip losses were also ignored, so the expression for C_Q is (66) with $K = 1.0$, $V_c = 0$ and $B = 1.0$, i.e.,

$$C_Q = \frac{(C_T)^{\frac{3}{2}}}{\sqrt{2}} + \frac{\sigma \delta_0}{8} + \frac{2}{3} \cdot \frac{\delta_1}{a} \cdot C_T + \frac{4 \delta_2}{\sigma a^2} \cdot C_T^2 \dots(67)$$

In an Appendix to the paper, expressions are given for the optimum blade defined as one which will produce a given thrust for the least power expenditure. In practice the optimum is closely approached by a blade which has uniform inflow over the disc and in which each section is operating at the angle of attack giving the least profile drag losses.

For such a rotor the twist and taper are given by:

$$\theta_x = \alpha_x + \frac{v}{x \Omega R} \dots(68)$$

$$c = \frac{c_t}{x} \dots(69)$$

where α_x and v are constant by definition and c_t is the tip chord.

The performance of the optimum blade is derived in the Appendix as:-

$$C_Q = \frac{(C_T)^{\frac{3}{2}}}{\sqrt{2}} + \frac{\sigma c_{d_0}}{9} \dots(70)$$

Tables IV and V present the results of the analysis at two values of C_Q .

Table IV

Effect of Combined Twist and Taper on Hovering Performance

Linear Blade Twist Degrees	Blade Taper (Ratio of Root Chord to Tip Chord)	Percentage Thrust Increase	
		$C_Q = 0.00026$	$C_Q = 0.00044$
<u>Twist Without Taper</u>			
0	1	-	-
-8	1	2	3
-12	1	3	4
Ideal	1	5	5
<u>Twist With Taper</u>			
0	3	-	-
-8 and -12	3	3	2
<u>Taper Without Twist</u>			
0	1	-	-
0	3	2	3
<u>Taper With Twist</u>			
-12	1	-	-
-8 and -12	3	1	1

Table V/

Table V

Increase in Hovering Thrust as Compared with the Thrust of
an Untwisted Rectangular Blade

Linear Blade Twist Degrees	Blade Taper (Ratio of Root Chord to Tip Chord)	Increase in Thrust Over Untwisted, Untapered Blade Percentage	
		$C_Q = 0.00026$	$C_Q = 0.00044$
0	1	-	-
-8	3	5	5
-12	3	5	5
Ideal	Optimum	7	7

Partial Taper In conventional blades the taper usually extends from the tip to about one half of the radius, the part inboard being rectangular. To determine whether such partial taper reduced hovering efficiency, calculations were also made for a blade tapered only over the outer half the taper (3) being reckoned on the root chord obtained by extending the leading and trailing edges of the tapered part to the root. Little difference was found between this and a fully tapered blade of the same taper ratio and solidity.

Solidity The results summarized in Tables IV and V refer to rotors of solidity 0.06. The calculations were repeated for rotors of 0.042 solidity and in general lead to the same conclusions.

3.2 Full Scale Tests in Forward Flight

3.21 Tunnel Tests

Ref. 29 gives the results of tests in the full scale tunnel on the YR-4B helicopter equipped with two rotors, one the production type flight tested in Ref. 20, the other a smooth set of blades.

Unfortunately the production set of blades was only tested over a range of tip speed ratio from $\mu = 0.17$ to $\mu = 0.20$ so that there are only a few flight tests which can be compared directly with the tunnel figures. Over this range the rotor power from flight tests is appreciably higher than indicated by the tunnel tests.

The tests on the two rotors are however strictly comparable and, again over the restricted range of overlap of the tests, do give an indication of the lower profile drag of the smooth blades. On the average the drag/lift ratio of the production blades is 22% higher than that of the smooth blades giving confirmation of the difference shown in the basic drag/lift curves of Fig. 7.

While this report has not been analyzed in detail because of the wider range of the flight tests it is of great value as giving lift, drag and pitching measurements of the fuselage for use in the subsequent analysis.

3.22 Flight Tests

Refs. 30 and 21 give the results of flight tests on the YR-4B helicopter, the first with the production fabric covered blades and the second with an alternate set of blades of reduced solidity, with smooth plywood cover and of NACA 23015 section instead of the NACA 0012 used on the production blades.

These reports are of the greatest value from the point of view of the major purpose of the present investigation, since the power distribution is given in full detail, as well as c.g. position, cyclic pitch control to trim, etc., so that the fullest analysis is possible.

3.221 Variation in Effective Blade Drag with Forward Speed

As has been pointed out earlier the mean effective drag coefficient in forward flight is related to the mean drag coefficient when hovering by three factors dependent one on tip speed ratio alone and the other two on the combination of tip speed and forward speed.

3.2211 Variation in Effective Blade Drag with Tip Speed Ratio $(f)_\mu$

The mean blade drag is a function of the lift distribution across the disc and increases as the tip speed ratio increases, though this increase has been ignored by all writers on performance estimation with the sole exception of Talkin¹.

Fig. 8 gives the factor $(f)_\mu$ by which the "basic" (i.e., hovering) drag coefficient must be increased to give the mean effective drag over a range of μ values. The curve of Fig. 8, which has been in use, and given satisfactory profile drag power estimates, for many years was originally derived by integrating over the disc for a number of rotors covering the commonly used range of design parameters.

In the course of the present analysis all available tests, within the range where tip stalling was absent have been analysed, and further integrations for modern helicopters have been made. This new analysis confirms the curve which is presented in its original form.

3.2212 Compressibility Correction $(f)_\mu$

In the past attention has been drawn to the fact that normal methods of performance estimation for helicopters, even with the correction $(f)_\mu$, appreciably underestimate the power required. Several correcting factors have been proposed from time to time but these when adjusted to fit the measured performance of one helicopter could not be applied satisfactorily to a different design. This was particularly the case with the Bristol Type 171 whose rotor is operating at a higher tip speed than the very few other helicopters available for analysis. Unfortunately in the past it has usually been assumed that so long as the relative speed of the advancing blade $(V + \Omega R)$ did not exceed about 0.8 of the speed of sound there would be no drag rise due to compressibility. During the course of the present investigation the conclusion was reached that the discrepancy between estimated and measured performance of the Bristol Type 171 could only be due to a compressibility effect, and a simple method of obtaining a correction was sought.

Ref. 31 gives the results of an investigation carried out under static conditions on two full scale rotors, differing only in that one set of blades was untwisted while the other set had 8° negative twist. Curves are presented showing the critical combinations of tip speed and tip angle of attack at which compressibility losses are encountered, and the rate of increase of these losses with tip angle of attack as measured by the ratio of measured to the theoretical profile drag torque.

In general, once the critical combination of tip speed and tip angle of attack is exceeded the ratio of measured to calculated profile drag torque coefficient approximately doubles for an increase in tip angle of attack of 2°. This result of course applies only to hovering where the blade is equally influenced round the whole disc. In forward flight however the rate of growth of the compressibility losses will vary with flight conditions. The author suggests that the rate of growth may lie between the rate of growth of stalling losses in forward flight (see para. 3.2213) and the rate of growth of compressibility losses in hovering. Even with high performance helicopters however the tip angle on the retreating side is not likely to be permitted to rise much above 12° at normal operating speeds, due to the onset of vibration and loss of control, and for this angle the limiting tip speed at which losses begin to be encountered is about 350 ft/sec. Such a type might have a rotor operating at about 750 ft/sec tip speed, and to have 350 ft/sec relative speed on the retreating blade would involve a forward speed of 400 ft/sec, which would appear to be outside the bounds of practicability for a conventional helicopter, even with stub wings to lower the rotor operating C_T at high forward speed. Moreover such a type would have blade sections much thinner than the tested blades which were of 15% thickness/chord ratio. In general then no compressibility losses are to be expected on the retreating blades, and it is suggested that a rate of growth of compressibility losses one half that disclosed by the tests would be nearer the truth. Such a rate of growth does in fact explain the discrepancy between estimated and measured tip speed of the Bristol Type 171 though somewhat high due presumably to the much thinner tip sections (7% thickness/chord ratio).

The tests however cannot easily be applied to routine performance calculations and the following method is suggested as adequate.

(a) Critical Blade Aerofoil Mach Number (M_C)

M_C at zero lift, in terms of aerofoil thickness/chord ratio is given in Fig. 9.

(b) Variation in M_C with Lift Coefficient

The tests of Ref. 31 give the variation in M_C with tip angle and this is in reasonable agreement with two-dimensional tunnel data. The tests however disclose that on twisted blades there is a slight delay in the onset of compressibility losses varying somewhat and equivalent to raising the effective angle of attack by from 0.5° to 1.5°. To make use of this in order to differentiate between twisted and untwisted blades the test results in conjunction with two-dimensional tunnel tests on the aerofoil have been used to prepare Fig. 10 which gives the ratio of the critical Mach number M_C^1 at various mean lift coefficients to the critical Mach number M_C at zero lift. The curves of variation of M_C^1 for different aerofoils all have the same general shape and the M_C curves given can be looked upon as being of general application.

(c) Tip Section Lift Coefficient

It is suggested that for routine estimation it is sufficiently accurate to base the compressibility correction on the mean advancing blade lift coefficient and Fig. 10 has been adjusted accordingly.

We can then write the mean advancing blade lift coefficient in terms of the mean hovering lift coefficient as:

$$\bar{C}_{L_{\text{advancing blade}}} = \bar{C}_{L_{\text{hovering}}} \cdot \left(\frac{1}{1 + \mu} \right)^2 \quad \dots (71)$$

(d)/

(d) Drag Rise Due to Compressibility - $(f)_c$

A generalized curve showing the compressibility drag factor against the ratio of M actual to M'_c critical is given in Fig. 11.

The process of estimating the compressibility factor $(f)_c$ is then:

- (1) From Fig. 9 read M_c at zero lift.
- (2) Estimate the mean advancing blade lift coefficient from (71).
- (3) At this lift coefficient read $\frac{M'_c}{M_c}$ from Fig. 10 and thence the M'_c applicable to the advancing blade.
- (4) Calculate the actual M of the advancing blade, i.e.,

$$\frac{V + \Omega R}{\text{speed of sound}}$$

- (5) Read the compressibility drag factor $(f)_c$ from Fig. 11 at the ratio of $\frac{M_{\text{actual}}}{M'_c}$.

In passing it is of interest to note that the tests of Ref. 31 at normal operating tip speeds used in the theoretical estimates show that 8° negative twist decreased the power required at normal thrust coefficients by about 3% as predicted in Table IV.

3.2213 Stalling Correction $(f)_s$

In Refs. 21, 32 and 33 plots are given of the ratio of measured to calculated rotor profile drag/lift ratio against calculated retreating blade tip angle of attack. These plots all of which were obtained on the YR-4B helicopter with varying sets of blades all show that the profile drag power begins to rise rapidly when the retreating blade tip angle of attack reaches 12° above no lift. Handling tests on the same helicopter (Ref. 34) have also shown that at this same angle of attack the pilot begins to experience vibration and control difficulty, the aircraft becoming virtually impossible to fly when 16° is reached.

The profile drag power plots indicate that between 12° and 16° the power required doubles. In the compressibility tests of Ref. 31 the losses at the lower tip speeds are predominantly stalling losses and here again at tip speeds of 350 to 400 ft/sec the onset of rise in profile drag torque occurs at calculated tip angles of 12°. The rate of growth of profile drag power however is not quite so great as that given by the flight test analyses. In the tests, which were made in the hovering condition, the profile drag power increased until at tip angles of 16° it was about three times the value at 12°. As only half the disc is affected in forward flight we can conclude that these tests indicate an increase of 1.5 times, rather than of 2.0 times as indicated by the flight test analyses. The flight test analyses are however open to some criticism to the extent that they are based on uniform induced velocity, and make no allowance for the changing lift and drag distribution over the disc with forward speed.

With/

With the methods of analysis of the present report, including the $(f)_{\mu}$ and, where appropriate, the $(f)_c$ correcting factors, a much lower rate of growth is indicated, and in any event the rate of growth of the NACA analyses results in considerable over-estimation of the power required at top speed by more modern helicopters than the YR-4B of the tests.

All available flight and tunnel tests both model and full scale have been analysed, and while there is considerable scatter in the test points the resulting mean curve is that presented in Fig. 12 which in association with the basic drag curves of Fig. 7 and the $(f)_{\mu}$ and $(f)_c$ corrections does give excellent agreement between measured and calculated performance for all the modern helicopters for which flight tests are available.

3.3 Full Scale Tests in Autorotative Glides

Two reports give tests in autorotative glides Ref. 35 on the YR-4B helicopter with the production fabric covered blades, and Ref. 21 with the alternative set of low solidity plywood covered blades. Using the same theory as for powered flight the derived effective mean blade drag coefficients show very pronounced scatter so that it is extremely difficult to say what is the mean basic drag curve applicable. The most that can be said is that for the fabric covered blades they would appear to be evenly distributed about a curve lying half way between the conventional rough and smooth blade curves of Fig. 7. For the plywood covered blades they are about 10% lower than the curve of Fig. 7. The apparently lower effective blade drag of these blades in autorotation as compared with level flight has previously been remarked by Sikorsky, who suggested that the drag coefficient at zero lift in autorotation is about 20% lower than that in powered flight.

The tests do however show clearly the benefits in reduced rate of descent in autorotation, which come from better surface and twist. For instance, at the tip speed for minimum rate of descent the alternate rotor drag/lift ratio is about 0.045 lower than that of the production rotor with fabric covered blades. This corresponds to a reduction of 160 ft/min, or some 16% decrease, from the 1085/min measured on the original rotor at a forward speed of 40 miles per hour at a gross weight of 2565 pounds.

3.4 The Effects of Blade Twist

Ref. 33 repeats the level speed tests of Ref. 21 with a rotor of the same dimensions and surface finish but without twist.

Estimates of the power required made by the methods of the present report agree very well with the measured performance when the smooth basic drag curve of Fig. 7 is used.

Comparative curves are presented showing the ratio of the measured rotor profile drag/lift ratio to the estimated value, plotted against retreating blade tip angle of attack and as discussed in para. 3.221/ again show an apparent doubling of profile drag power as the tip angle increases from 12° to 16° .

There is a discrepancy in the results from the untwisted and twisted blades to the extent that while the rate of growth in profile drag power is the same, the onset of the drag rise occurs about $1\frac{1}{4}^\circ$ later for the untwisted blades. The two curves should coincide and the discrepancy must be attributed to errors in calculating the tip angles.

A plot is given comparing the two sets of tip angles of attack for the test aircraft at the same operating conditions and over a range of forward speeds. This shows that for the blades with 8° negative twist the tip angles of attack are about 2.5° less than for the untwisted blades. The range of tip speed ratio covered is from 0.125 to 0.25. Over this range the expression (48) and the inset curve on Fig. 3 show a reduction of from 2° to 2.3° .

The effectiveness of blade twist in extending the speed range of helicopters is demonstrated and shows that tip losses begin at a speed of 7 miles per hour (i.e., about 10%) higher on the test helicopter with the twisted blades. The comparison also shows that once stalling has developed the twisted blades required approximately 15 h.p. less to operate at the same speed.

A comparison between the two rotors in vertical autorotative descent is also given. The test data show that negative twist does not affect the effectiveness of a rotor in vertical autorotative descent.

3.5 Blade Flapping and Control to Trim

Ref. 21 gives centre of gravity position, stick position to trim as well as fuselage and no-feathering axis attitude and this permits analysis of control to trim and flapping.

Ref. 36 gives measurements of blade motion, and the results of harmonic analysis to give the flapping and feathering coefficients in the Fourier Series.

The analysis of the material in these reports confirms all past experience from both model and full scale tests on both helicopters and autogiros, vide for example Refs. 12, 15 and 18, that theory underestimates the flapping angles, and therefore also underestimates the control applied cyclic pitch to trim.

Theory estimates the shaft and disc attitude with good agreement with flight measurements.

In Ref. 36 the centre of gravity position is not recorded but the fuselage pitching moment curve derived from the tests of Ref. 21 permits a reasonable estimate. The estimates derived in this way agree well with the author's own estimates quoted in the paper. The range of operating conditions and c.g. positions in these tests is so wide that a plotted comparison between theory and experiment is hardly possible. A typical comparison however is given below.

Weight	Estimated from C_T 2850 lb
Speed	106 ft/sec
Tip speed ratio	0.22
C.g position	Estimated 2.4" forward of shaft

	Estimated values	Measured values
α	6.1°	6.41°
α_s	7.4°	7.4°
α_{is}	1.3°	0.99°
α_i	3.5°	5.17°
B_{is}	2.2°	4.2°
α_{nf}	9.6°	11.6°
α_{nf} (from estimated λ_{nf})	9.6°	

The main interest in Ref. 36 however is in the analysis of the in-plane blade motion. The mean lag angle of a blade is essentially a function of the shaft torque in-put divided by the square of the angular velocity, and the author contents himself with plotting the values of the ratio of rotor shaft power to the cube of the rotor

rotational speed $\left(\text{which ratio is proportional to } \frac{Q}{\Omega^2} \right)$ against measured lag angles.

The results plotted in this way do fall on a straight line showing that a mechanical device measuring mean lag angle could be calibrated and used as a torquemeter.

The mean lag angle in radians is given to a close approximation by

$$\gamma_0 = \frac{Q}{be (M \Omega^2 r_{og}) \left(\frac{e}{r_{df}} + 1 \right)} \quad \dots(72)$$

where γ_0 is the lag angle.

Q the rotor shaft torque in-put in lb/ft.

b the number of blades.

e the distance from drag hinge to centre of rotation.

M the blade mass in slugs.

r_{og} the radial position of the blade c.g. from the drag hinge in ft.

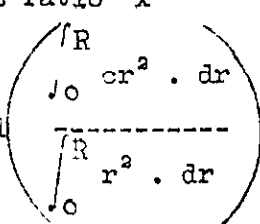
r_{df} the radial position of the resultant drag force from the drag hinge in ft.

Inserting the values for the test blades (72) can be rewritten in terms of the operating parameters as:

$$\gamma_0 = \frac{\frac{P}{L} \times V \times C_T \times 31.5}{\Omega} \quad \dots(73)$$

Expression (73) consistently underestimates the test lag angles by 6%, and if we use 94% of the measured lag angle in the expression we get absolute agreement with the measured $\frac{P}{L}$ values in the flight tests, and the same values for the rotor mean profile drag coefficient as in the other analyses.

List of Symbols

<u>Symbol</u>	<u>Quantity</u>	<u>Units</u>
a	Slope of lift coefficient against blade section angle of attack. Taken in this paper as 5.6	per radian
b	No. of blades per rotor	
B	Tip loss factor	
c	Local blade chord	ft
c_x	Blade chord at radius ratio x	ft
c_e	Effective blade chord 	ft
c_{d_0}	Blade element profile drag coefficient	
C_L	Rotor lift coefficient referred to disc area $\frac{L}{\frac{1}{2} \rho V^2 \pi R^2}$	
\bar{C}_L	Mean blade lift coefficient in hovering	
D	Drag	lb
f	Fore and aft position of centre of gravity relative to shaft. Positive behind shaft	ft
$(f)_i$	Variation of induced drag with forward speed	
$(f)_\mu$	Variation of effective blade mean drag coefficient with tip speed ratio	
$(f)_c$	Variation of effective blade mean drag coefficient with compressibility	
$(f)_s$	Variation of effective blade mean drag coefficient with retreating blade stalling	
$\left(\frac{D}{L}\right)_p$	Rotor profile drag/lift ratio	
$\left(\frac{D}{L}\right)_f$	Parasite drag of fuselage, rotorhead, blade shanks, etc. divided by rotor lift	
$\left(\frac{D}{L}\right)_i$	Rotor induced drag/lift ratio	

$$\left(\frac{D}{L}\right)_c$$

<u>Symbol</u>	<u>Quantity</u>	<u>Units</u>
$\left(\frac{D}{L}\right)_c$	Drag/lift ratio representing angle of climb	
$\left(\frac{D}{L}\right)_t$	Equivalent drag contribution of tail rotor divided by main rotor lift	
$\left(\frac{P}{L}\right)$	Shaft power parameter, where P is equal to the drag force equivalent to the shaft power at the velocity of flight	
h	Distance of rotor head above centre of gravity	ft
H	Longitudinal rotor force	lb
L	Lift	lb
M	Mach number	
M_f	Aerodynamic pitching moment of the fuselage	lb/ft
P	Rotor power	ft/lb/sec
P_i	Rotor induced power	ft/lb/sec
P_p	Rotor profile drag power	ft/lb/sec
HP	Rotor power	Horse power
HP_i	Rotor induced power	Horse power
HP_p	Rotor profile drag power	Horse power
Q	Rotor shaft torque	lb/ft
r	Distance of blade element from centre of rotor	ft
R	Radius of rotor	ft
x	Blade element radius ratio $\left(x = \frac{r}{R}\right)$	
T	Thrust	lb
V	Velocity along the flight path	ft/sec
V_c	Rate of climb	ft/sec
v	Induced velocity	ft/sec
v_c	Induced velocity in vertical climb	ft/sec
v_h	Induced velocity hovering	ft/sec
v_r	Induced velocity at radius r	ft/sec
v_t	Induced velocity at blade tip	ft/sec
		$v_x/$

<u>Symbol</u>	<u>Quantity</u>	<u>Units</u>
v_x	Induced velocity at radius ratio x	ft/sec
w	Disc loading $\left(\frac{W}{\pi R^2} \right)$	lb/sq ft
W	Weight of helicopter	lb
δ	Mean blade profile drag coefficient	
μ	Tip speed ratio $\left(\frac{V \cos \alpha}{\Omega R} \right)$	
α	Angle of attack of rotor disc, i.e., angle between rotor disc and flight path, positive when rotor tilted backwards	radians
α_s	Shaft "angle of attack", i.e., angle between shaft and the normal to flight path	radians
α_{nf}	"Angle of attack" of the axis of no-feathering, i.e., angle between axis of no-feathering and the normal to flight path	radians
α_x	Blade element angle of attack at radius ratio x measured from zero lift	radians
θ	Rotor blade pitch angle	radians
θ_o	Blade pitch at root	radians
θ_1	Linear blade twist from root to tip	radians
θ_m	Mean blade pitch at 0.75 radius	radians
λ	Inflow ratio relative to the disc axis (negative in helicopter powered flight), $\left(\frac{V \sin \alpha + v}{\Omega R} \right)$	
λ_{nf}	Inflow ratio relative to the no-feathering axis	
ρ	Air density	slugs/cu ft
ρ_o	Air density at sea level in standard atmosphere	slugs/cu ft
σ	Rotor solidity $\left(\frac{bc_c}{\pi R} \right)$	
Ω	Angular velocity of rotor	radians/sec
ΩR	Tip speed of rotor	ft/sec

<u>Symbol</u>	<u>Quantity</u>	<u>Units</u>
C_{Q_i}	Rotor induced torque coefficient $\left(\frac{Q_i}{\rho \cdot \pi R^2 \cdot (\Omega R)^2 R} \right)$	
C_{Q_p}	Rotor profile drag torque coefficient $\left(\frac{Q_p}{\rho \cdot \pi R^2 \cdot (\Omega R)^2 R} \right)$	
C_Q	Rotor torque coefficient $(C_{Q_i} + C_{Q_p})$	
C_T	Rotor thrust coefficient $\frac{T}{\rho \cdot \pi R^2 (\Omega R)^2}$	
ϕ	Inflow angle	radians
ϕ_x	Inflow angle at radius ratio x	radians
τ	Angle of flight path to horizontal	radians
a_1	Coefficient of $\cos\psi$ in the Fourier Series for flapping in the plane perpendicular to the no feathering axis. The longitudinal angle between the rotor disc axis and the no-feathering axis	
a_{1s}	Coefficient of $\cos\psi$ in the Fourier Series for flapping in the plane perpendicular to the rotor shaft. The longitudinal angle between the rotor disc axis and the shaft	radians
B_{1s}	Coefficient of $\sin\psi$ in the Fourier Series for feathering. The angle between the shaft and the axis of no-feathering	

References

<u>No.</u>	<u>Author</u>	<u>Title</u>
1	Talkin	Charts for helicopter performance estimation. N.A.C.A. A.C.R. No. L5E04.
2	Wald	A method for rapid estimation of helicopter performance. Journ. Aero. Sciences. April, 1943.
3	Castles	A direct method of estimating the performance of a helicopter in powered flight. Journ. Aero. Sciences. October, 1945.
4	Bailey and Gustafson	Charts for estimation of the characteristics of a helicopter rotor in forward flight. N.A.C.A. A.C.R. No. L4H07.
5	Liptrot	A comparison between measured and estimated helicopter performance. Unpublished A.R.C. 14,551 - H.133.
6	Brotherhood	An investigation in flight of the induced velocity distribution under a helicopter rotor when hovering. R.A.E. Report Aero 2212.
7	Glauert	Airplane propellers. Helicopter airscrews. Vol. 12 Aerodynamic Theory. Durand.
8	Brotherhood	Flow through helicopter rotor in vertical descent. R.A.E. Report Aero 2272.
9	Oliver	The low speed performance of a helicopter. A. & A.E.E. Report No. Res/264.
10	Brotherhood	An investigation in flight of the induced velocity distribution under a helicopter rotor when hovering. R.A.E. Report Aero 2212.
11	Montgomery Knight and Hefner	Static thrust analysis of the lifting airscrew. N.A.C.A. Technical Note No. 626.
12	Squire, Fain, and Eyre	Wind tunnel tests on a 12 ft diameter helicopter rotor. R.A.E. Report Aero 2324.
13	Glauert	A general theory of the autogyro. R. & M. 1111.
14	Lock	Further developments of autogyro theory. R. & M. 1127.
15	Wheatley	An aerodynamic analysis of the autogyro rotor. N.A.C.A. Report No. 487.
16	Bailey	A simplified theoretical method of determining the characteristics of a lifting rotor in forward flight. N.A.C.A. Report No. 716.
17	Lichten	Helicopter performance. Journ. Aero. Sciences. July, 1946.
18	Stewart	Helicopter control to trim in forward flight. R.A.E. Report Aero 2358.
19	Nikolsky and Seckel	Helicopter blade analysis. Princeton University. Report No. 100.

<u>No.</u>	<u>Author</u>	<u>Title</u>
20	Gustafson and Gessow	Flight tests of the Sikorsky YR-4B Helicopter II. Hovering and vertical flight performance. N.A.C.A. MR L5D09a.
21	Gustafson and Gessow	Analysis of flight performance measurements on a twisted plywood covered helicopter rotor in various flight conditions. N.A.C.A. Technical Note No. 1595.
22	Lipson	Static thrust investigation of full scale PV2 helicopter rotors having N.A.C.A. 0012.6 and 23012.6 aerofoil sections. N.A.C.A. MR No. L6D24.
23	Migotsky	Full scale tunnel tests of the PV2 helicopter rotor. N.A.C.A. MR L5C29a.
24	Dingeldein and Schaefer	Static thrust tests of six rotor blade designs on a helicopter in the Langley full scale tunnel. N.A.C.A. A.R.R. No. L5F25b.
25	Harrington	Full scale tunnel investigation of the static thrust performance of a co-axial helicopter rotor. N.A.C.A. Technical Note No. 2318.
26	Gustafson and Gessow	Effect of rotor tip speed on helicopter hovering performance and maximum forward speed. N.A.C.A. A.R.R. No. L6A16.
27	Gustafson	Effect on helicopter performance of modifications in profile drag characteristics of rotor blade airfoil sections. N.A.C.A. A.C.R. No. L4H05.
28	Gessow	Effect of rotor blade twist and plan form taper on helicopter hovering performance. N.A.C.A. Technical Note No. 1542.
29	Dingeldein and Schaefer	Full scale investigation of the aerodynamic characteristics of a typical single rotor helicopter in forward flight. N.A.C.A. Technical Note No. 1289.
30	Gustafson	Flight tests of the Sikorsky YR-4B helicopter I. Experimental data on level flight performance with original blades. N.A.C.A. MR No. L5C10.
31	Carpenter	Effects of compressibility on the performance of two full scale helicopter rotors. N.A.C.A. Technical Note No. 2277.
32	Gustafson and Gessow	Effect of blade stalling on the efficiency of a helicopter rotor as measured in flight. N.A.C.A. Technical Note No. 1250.
33	Gessow	Flight investigation of effects of rotor blade twist on helicopter performance in the high speed and vertical auto-rotative descent conditions. N.A.C.A. Technical Note No. 1666.
34	Gustafson and Myers	Stalling of helicopter blades. N.A.C.A. Technical Note No. 1083.

<u>No.</u>	<u>Author</u>	<u>Title</u>
35	Gessow and Myers	Flight tests of a helicopter in autorotation including a comparison with theory. N.A.C.A. Technical Note No. 1267.
36	Myers	Flight measurement of helicopter blade motion with a comparison between the theoretical and experimental results. N.A.C.A. Technical Note No. 1266.
37	Schaefer, Loftin, and Horton	Two dimensional investigation of five related N.A.C.A. airfoil sections designed for rotating-wing aircraft.

APPENDIX/

APPENDIX

Recommended Method for Helicopter Performance Estimation and
Comparison between Estimates and Measured Performance

1. Performance Estimation

All the well known methods for helicopter performance estimation are based on the same fundamental expressions for rotor induced and profile drag powers, and will give the same values if the various correcting factors of this report are applied.

Most of them, however, depend on some form of non-dimensional parameters in the calculations, and the power requirement in horsepower is not apparent until the final stages of the procedure.

The method suggested here is simpler and quicker in application, and has the merit of giving the power distribution directly in horsepower, so that the effect of changes in power due to changes in design, or in operating conditions, are immediately apparent. The tabulation is given below.

It should be pointed out that the expression given earlier for $(f)_i$, the correction for induced power for forward flight, is based on the flight velocity instead of the correct resultant velocity. It is a sufficiently good approximation at high forward speeds, but breaks down below about 60 ft/sec. Fig. 13 gives the correct values at slow speeds, $(f)_i$ being plotted against $\frac{v}{\sqrt{W}}$.

Tabular/

Tabular Performance Calculations	
Weight	W (lb)
Rotor diameter	(ft)
Disc area	A (sq ft)
Disc loading $\left(\frac{W}{A}\right)$	w (lb/sq ft)
Tip speed	ΩR (ft/sec)
$(\Omega R)^2$	(ft/sec)
$(\Omega R)^3$	(ft/sec)
Solidity	σ
$\frac{C_T}{\sigma} , \quad \frac{w}{\sigma \rho (\Omega R)^2}$	
Mean blade lift coefficient $\left(\frac{6.6 \times C_T}{\sigma}\right)$	
Mean blade profile drag coefficient δ	
Induced power hovering at sea level: Untwisted blades, $HP_i = 0.0303 \times W \times \sqrt{w}$ Twisted blades, 8° $HP_i = 0.0290 \times W \times \sqrt{w}$	
Profile drag power, hovering at sea level: $HP_p = \frac{\rho_o \sigma \delta \pi R^2 (\Omega R)^3}{4400}$	
Parasite drag at 100 ft/sec	D_{100} (lb)

Sea/

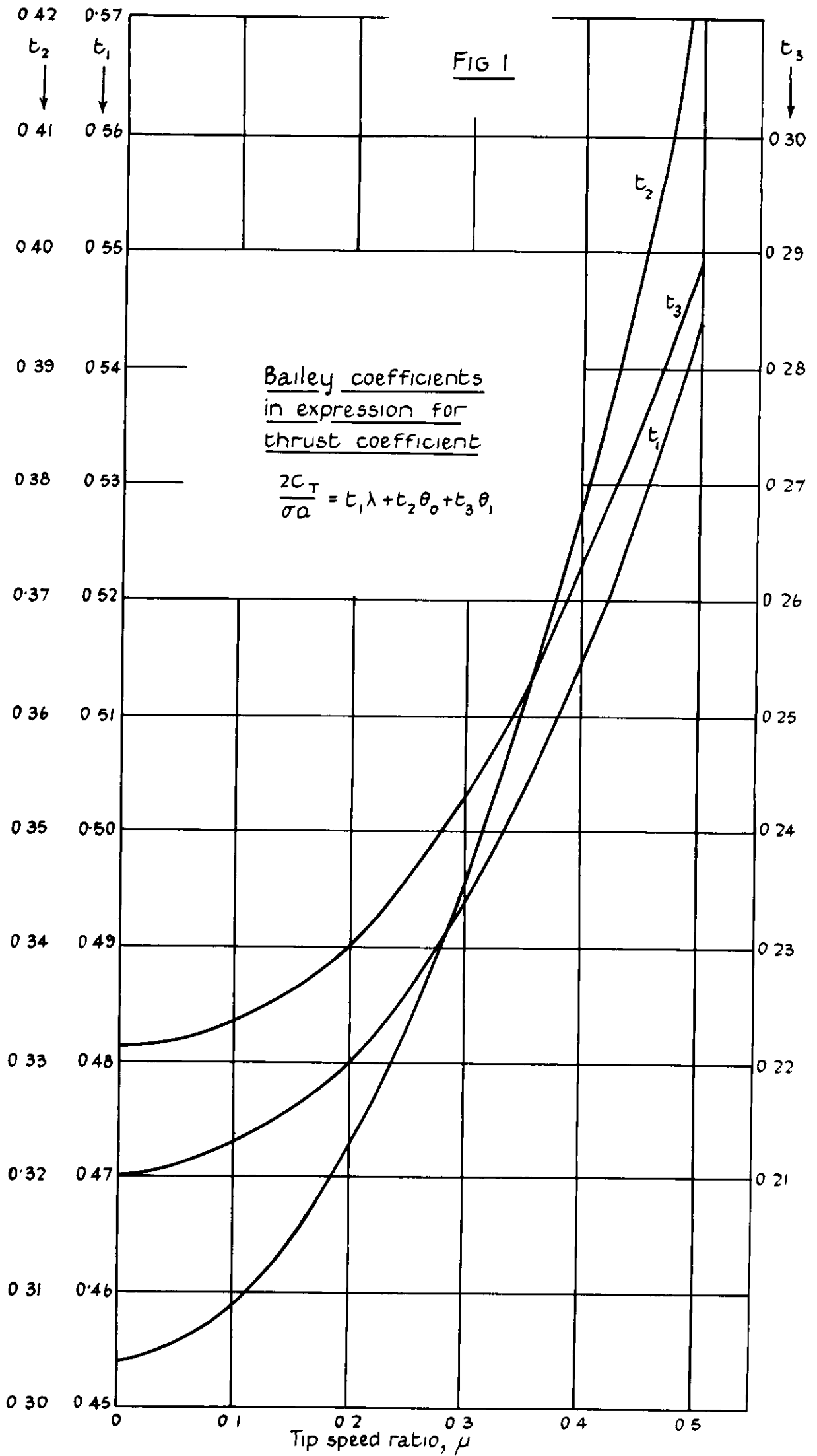
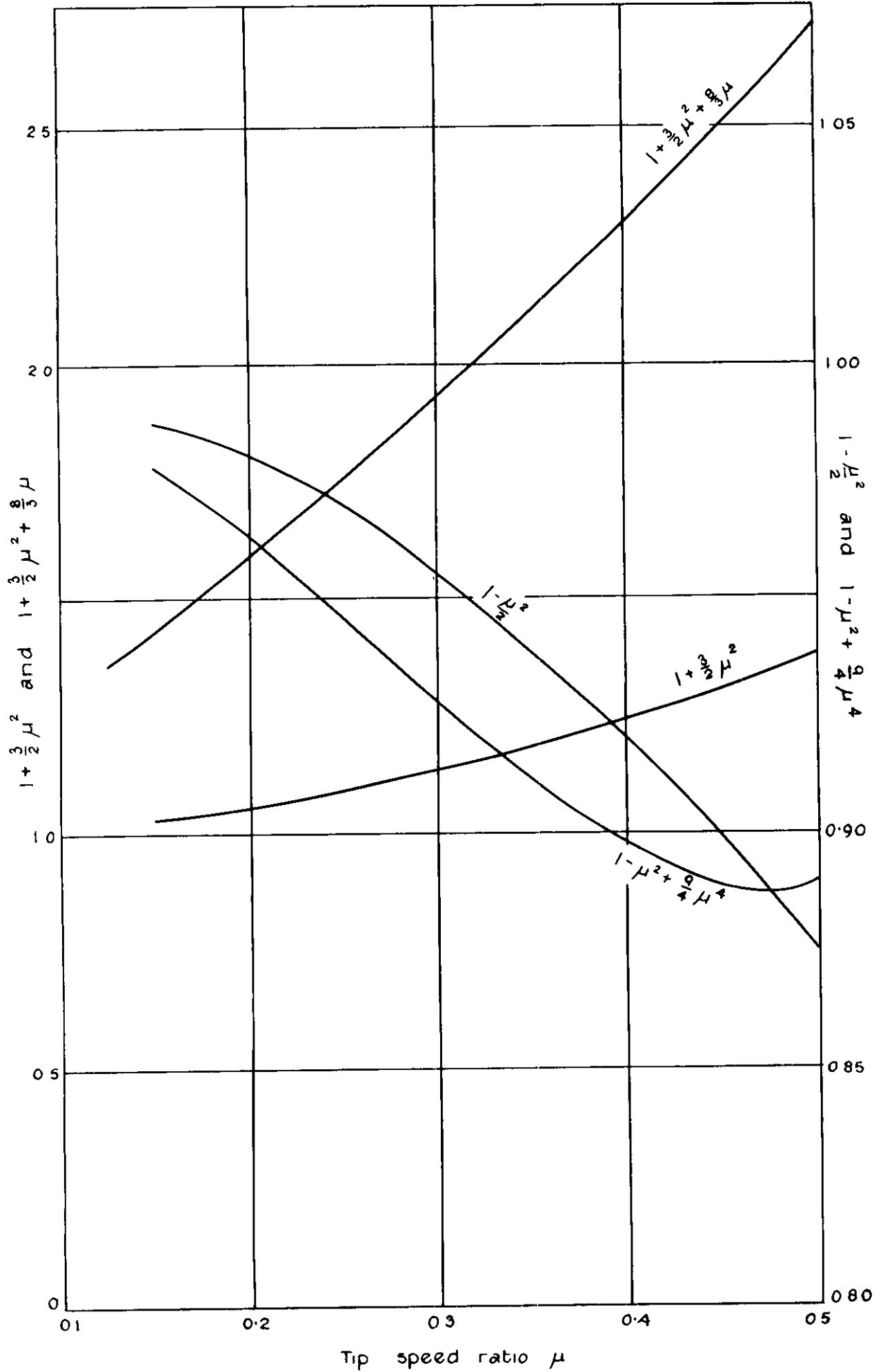


FIG 2



Standard terms in expression for maximum retreating blade tip angle of attack

FIG 3

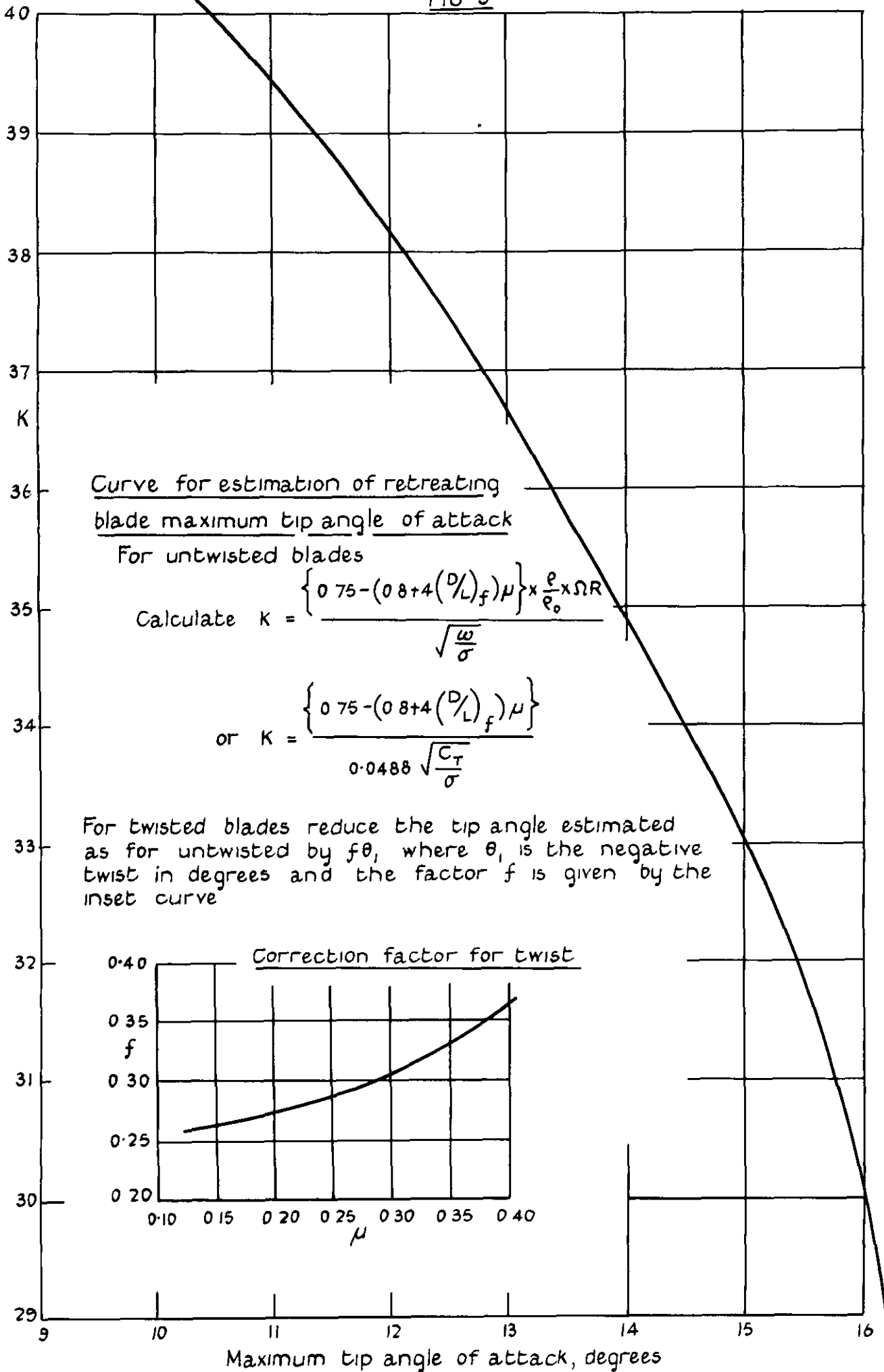
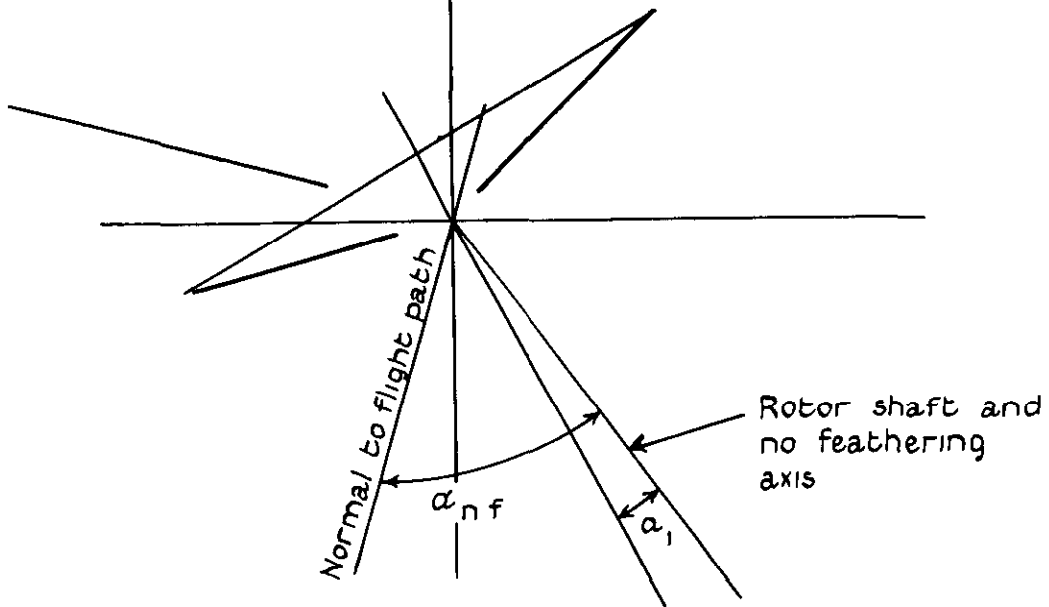
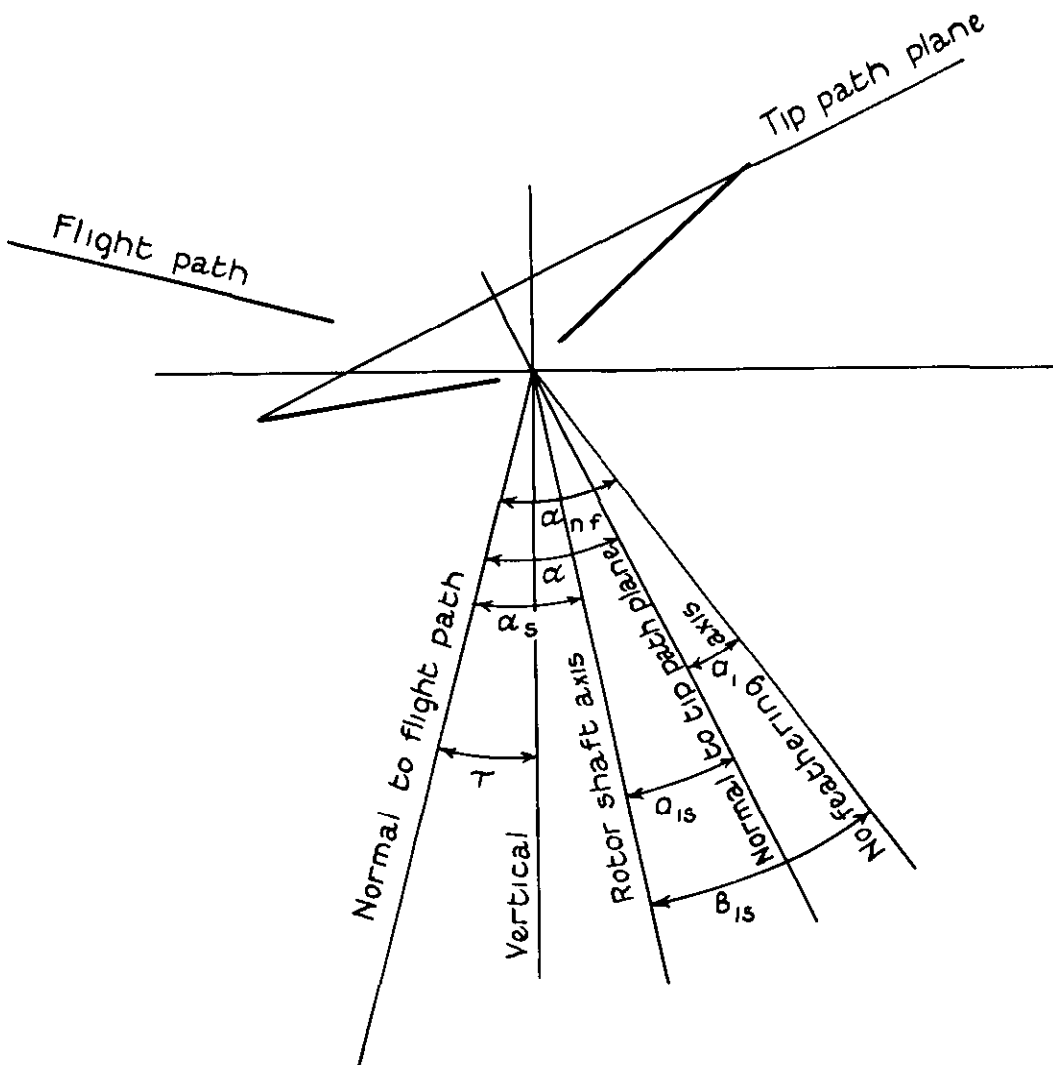


FIG 4.

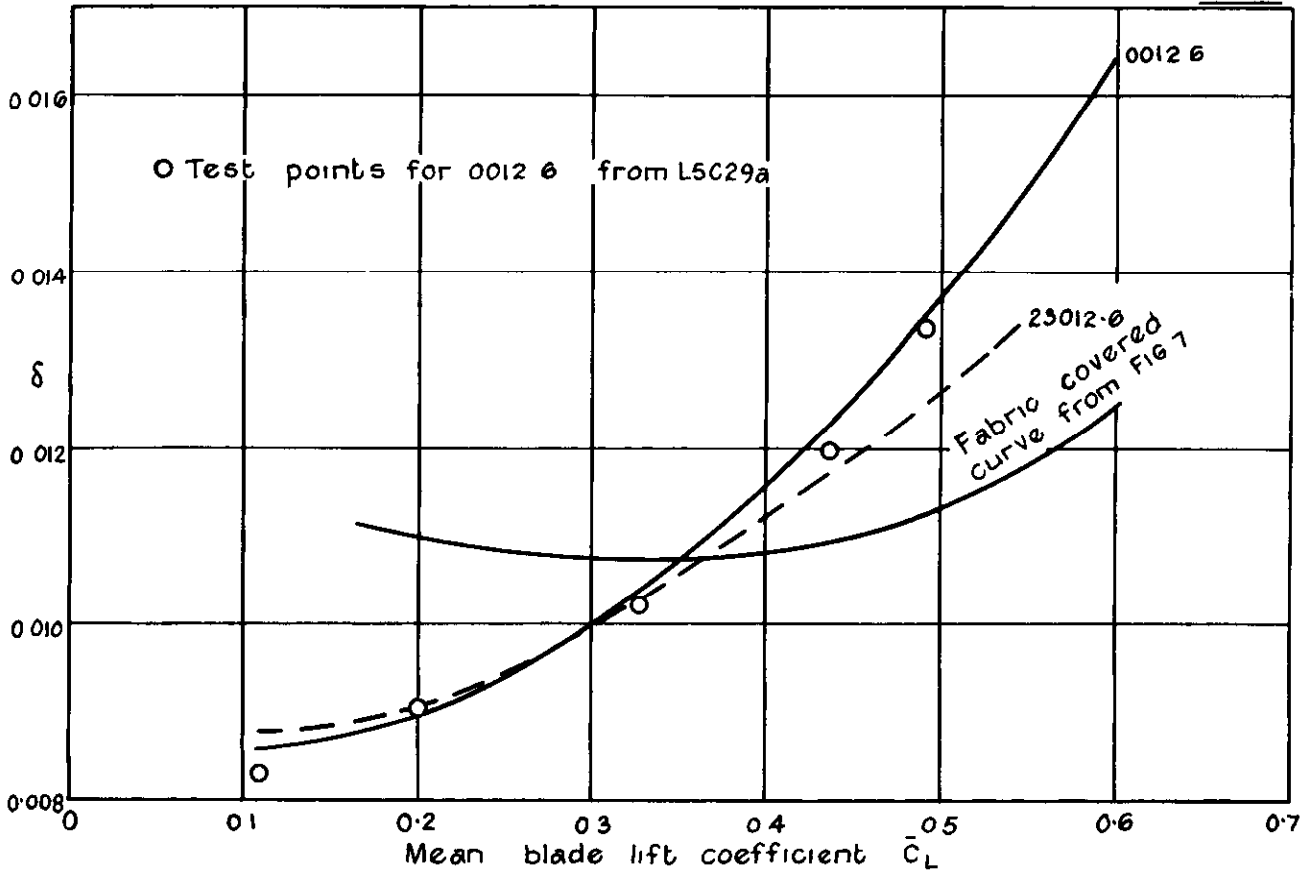


(a) Pure flapping system

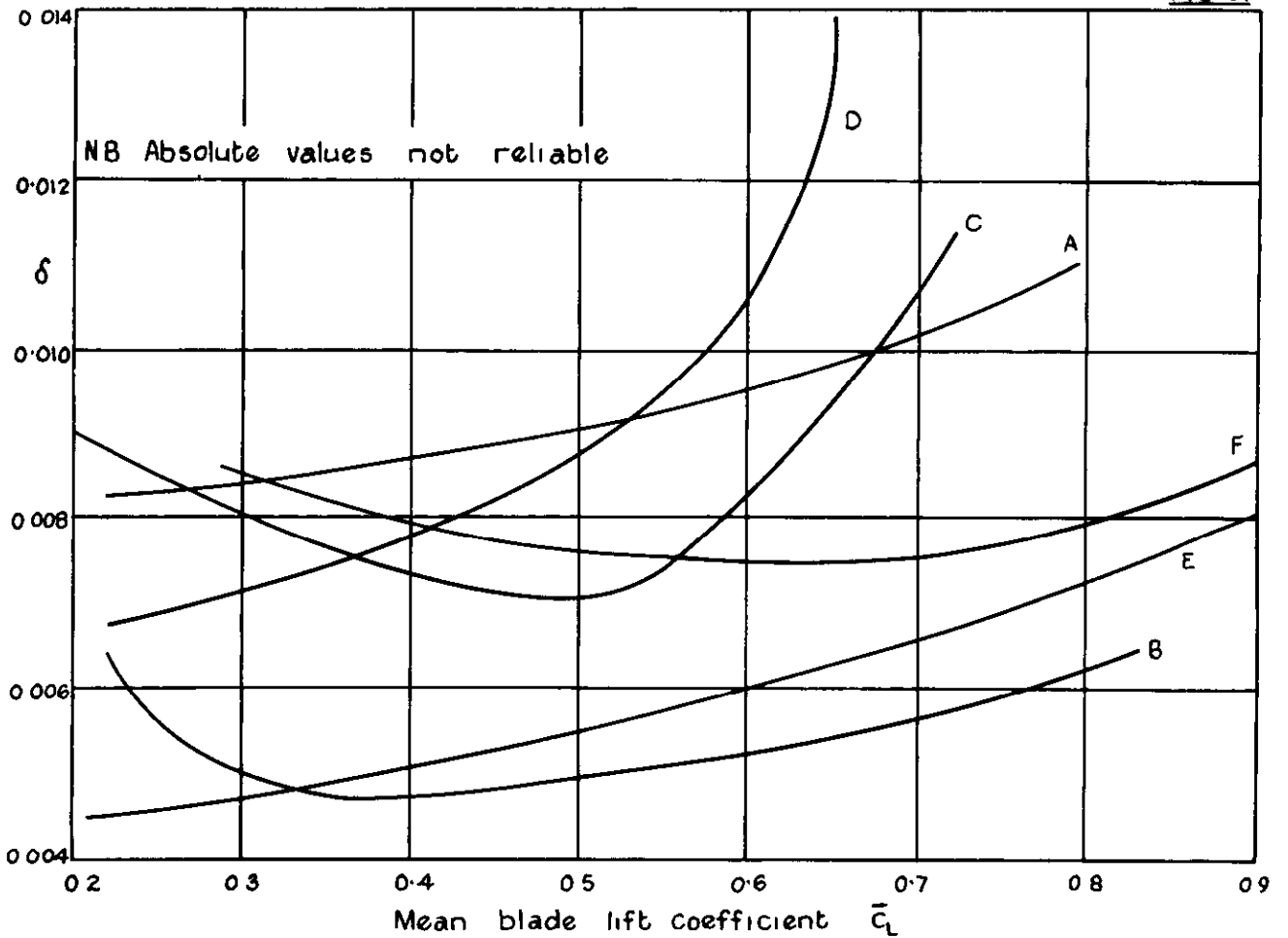


(b) System involving both flapping and feathering

Sketches showing the equivalence of a system involving both flapping and feathering as referred to the axis of no feathering, and a pure flapping system as referred to the rotor shaft



Mean drag/mean lift coefficient curves from full scale tunnel test on two fabric covered rotors having NACA 0012 δ and 23012 δ aerofoil sections. Reports MR, L6D24 and MR, L5C29 a



Mean drag/mean lift coefficient curves from full scale tunnel tests on six rotors. Report L5F25b

FIG 7.

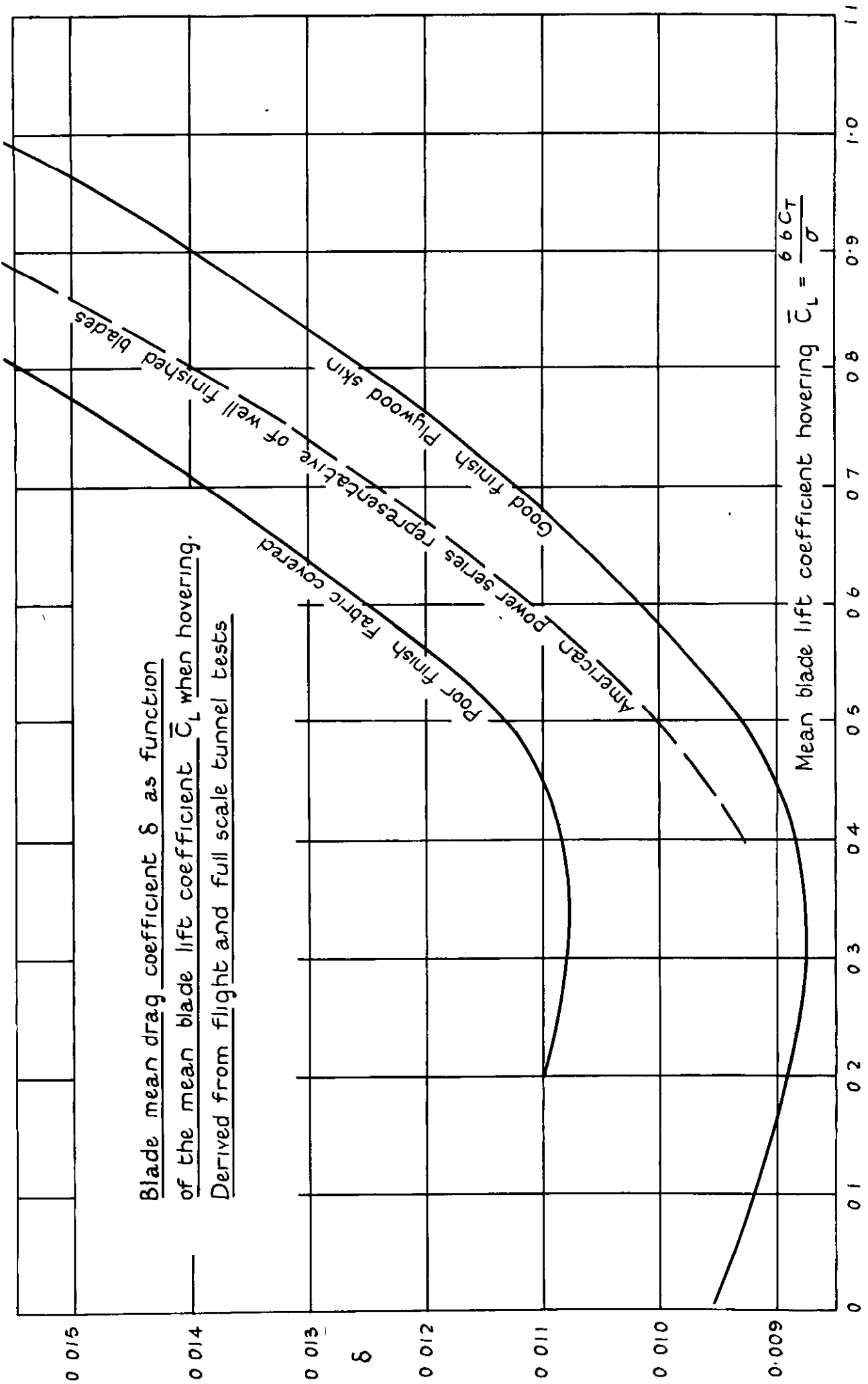
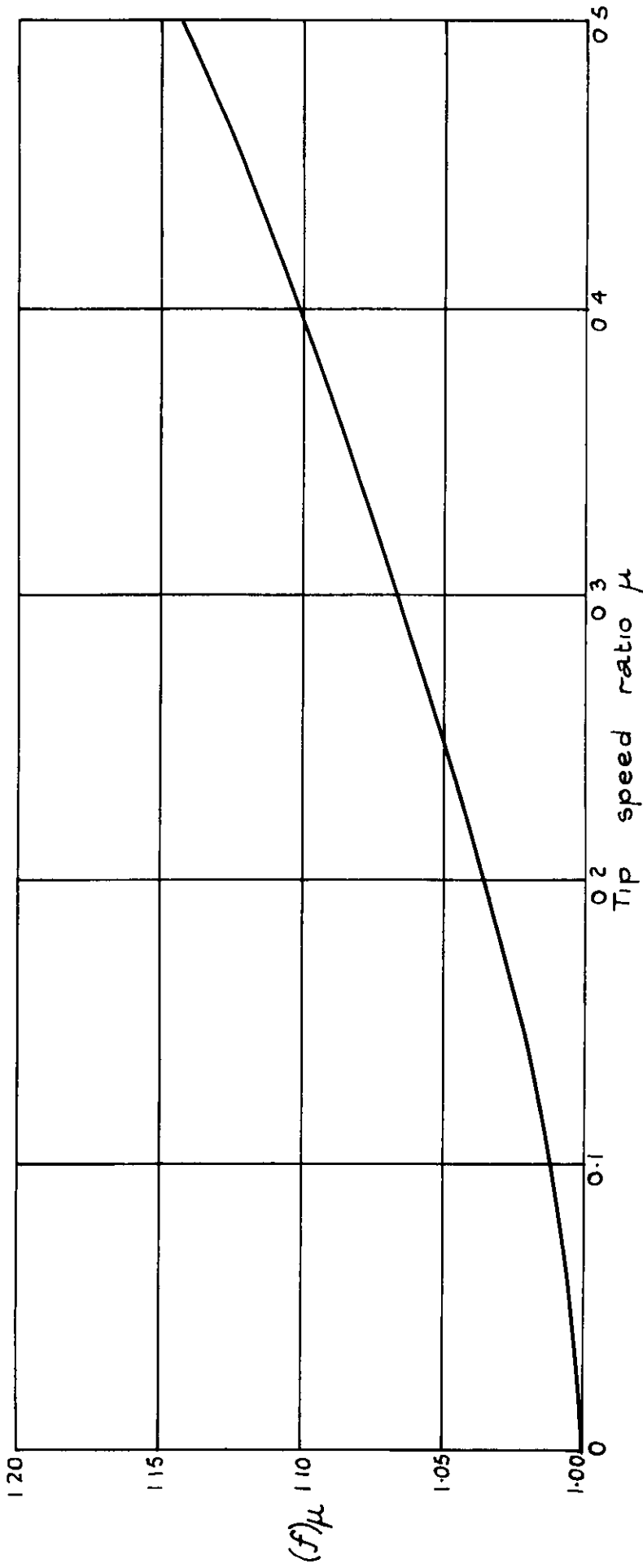


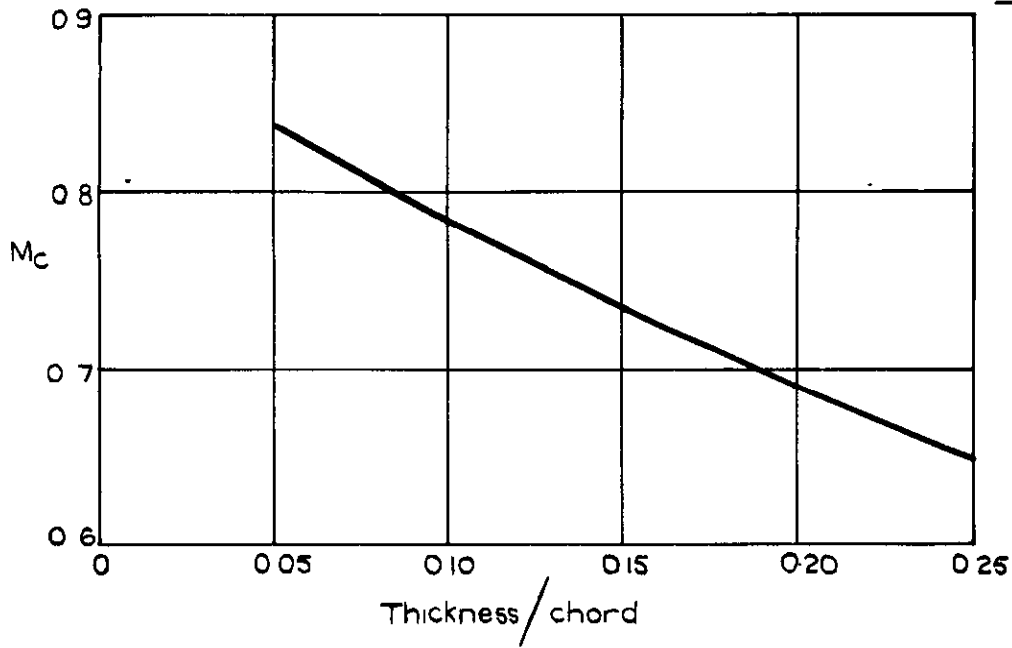
FIG 8.



Variation of effective blade mean drag coefficient with tip speed ratio
Curve of $(f)\mu$ against μ Equation to curve $(f)\mu = 1 + 0.4\mu^{1.5}$

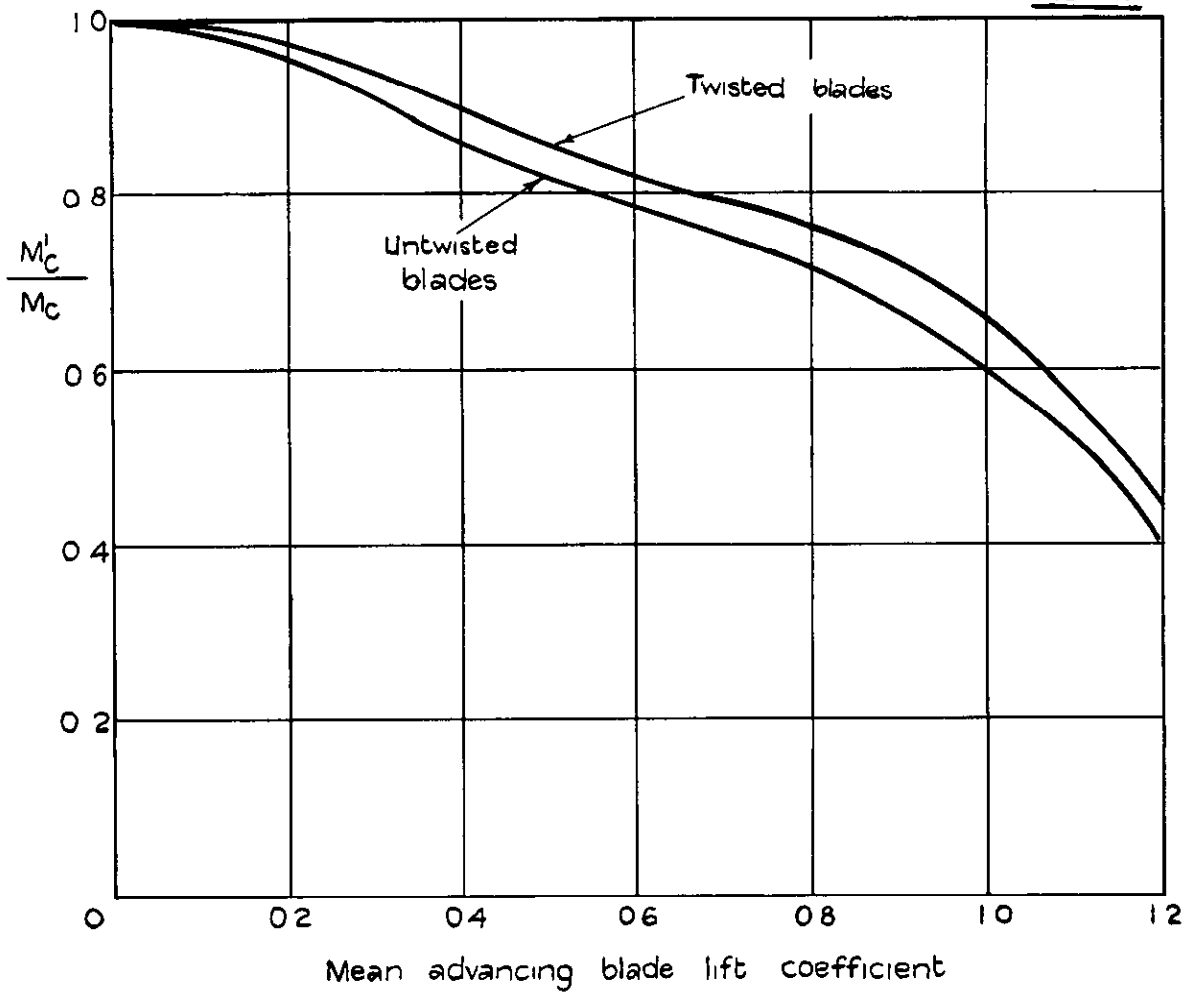
FIG 9 and 10.

FIG 9



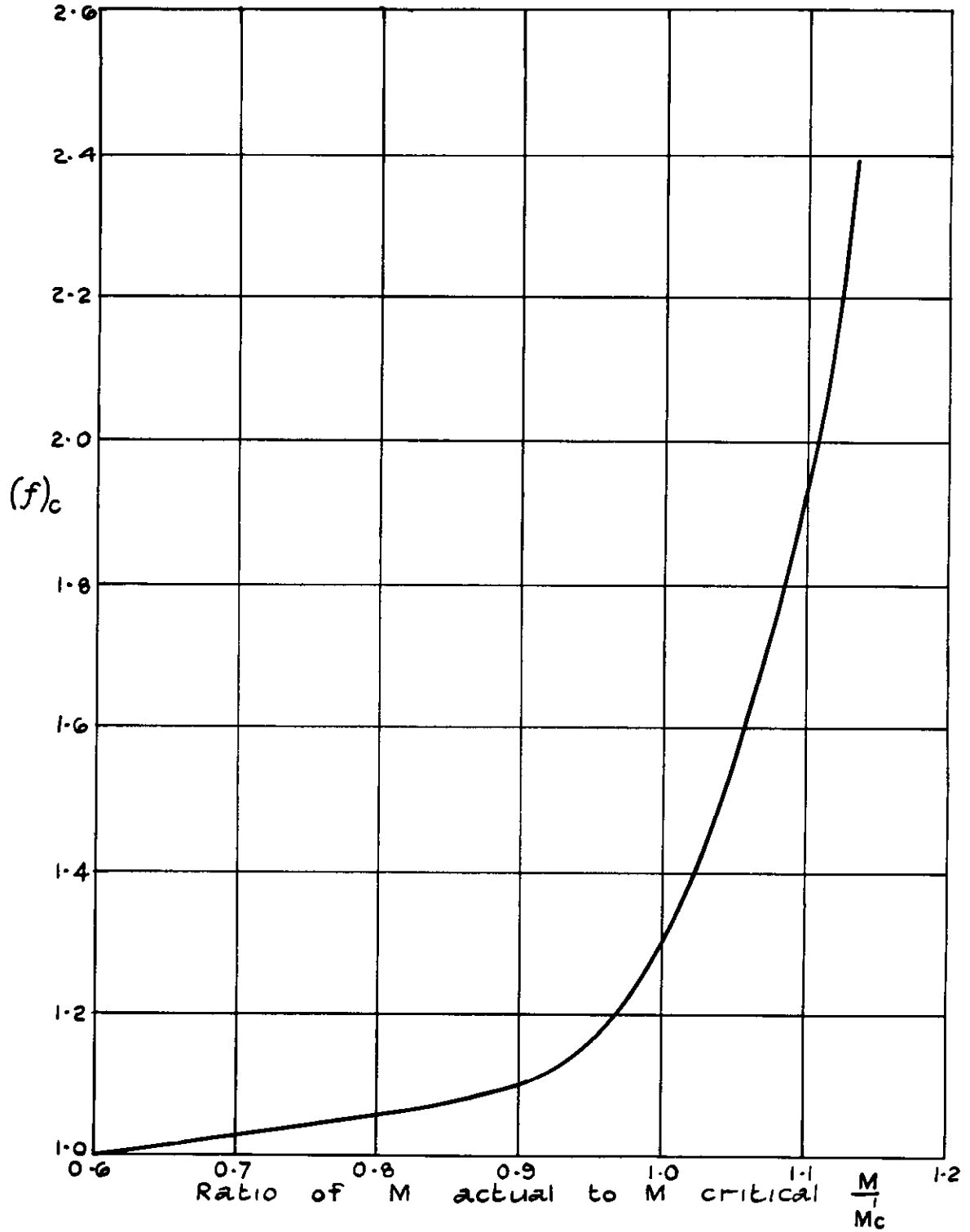
Aerofoil critical Mach number at zero lift as a function of thickness/chord ratio

FIG 10



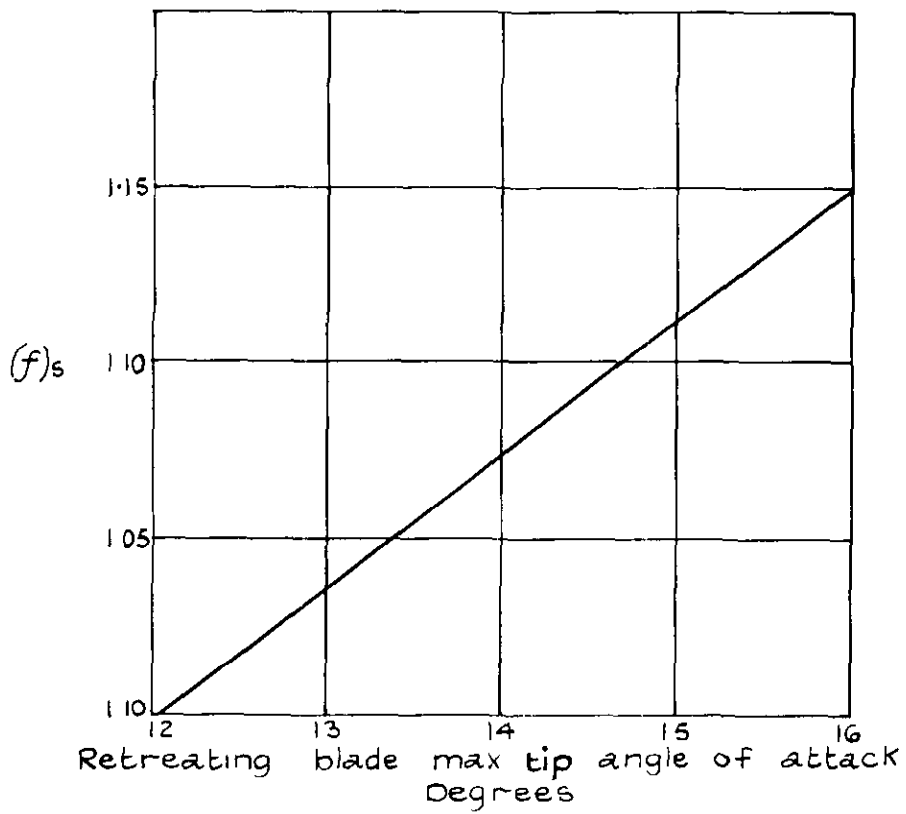
Variation of rotor blade critical Mach no with mean lift coefficient

FIG 11



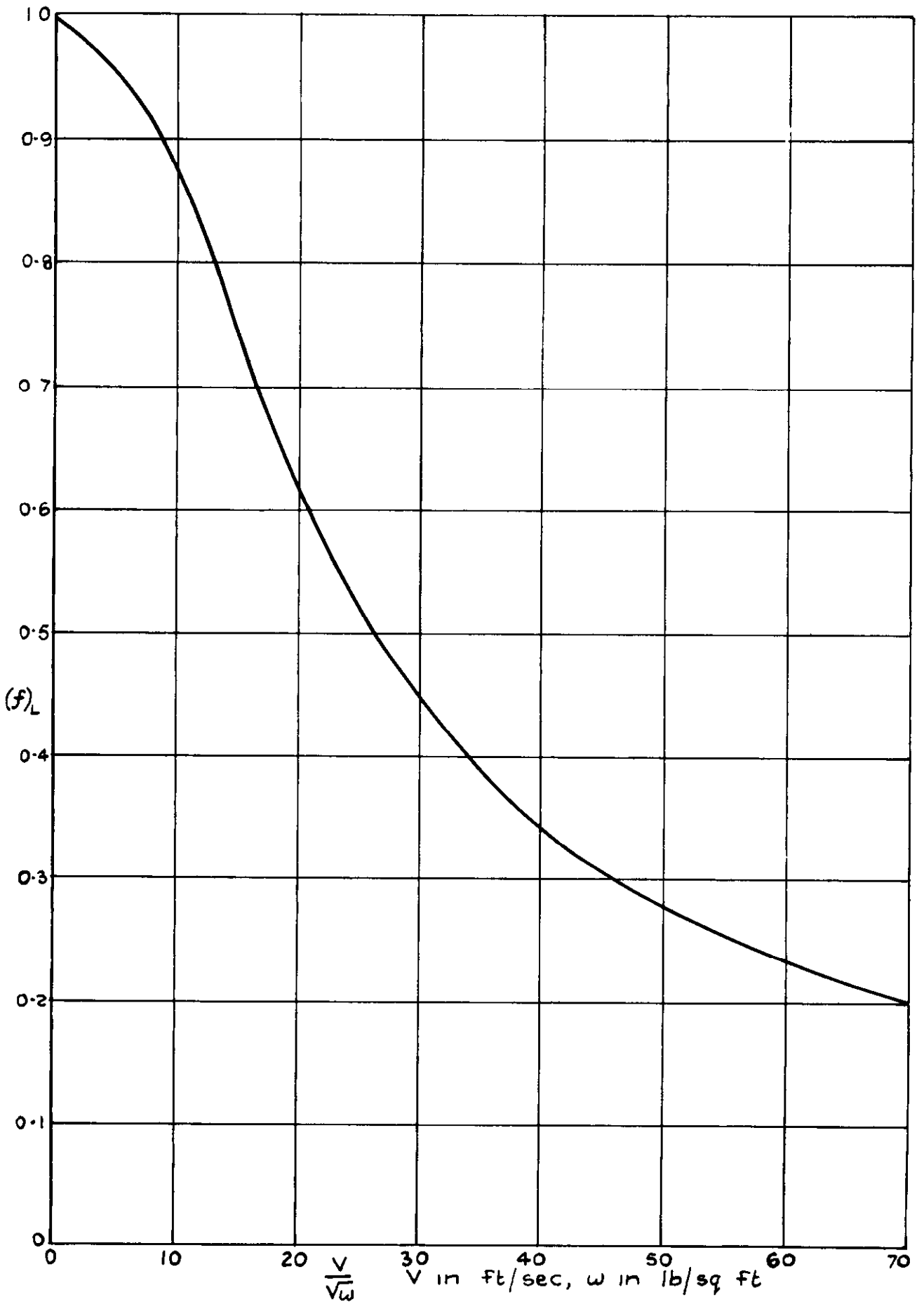
Variation of mean blade drag coefficient with compressibility effects.
Generalised curve of correcting factor $(f)_c$ against ratio of M actual to M critical

FIG 12



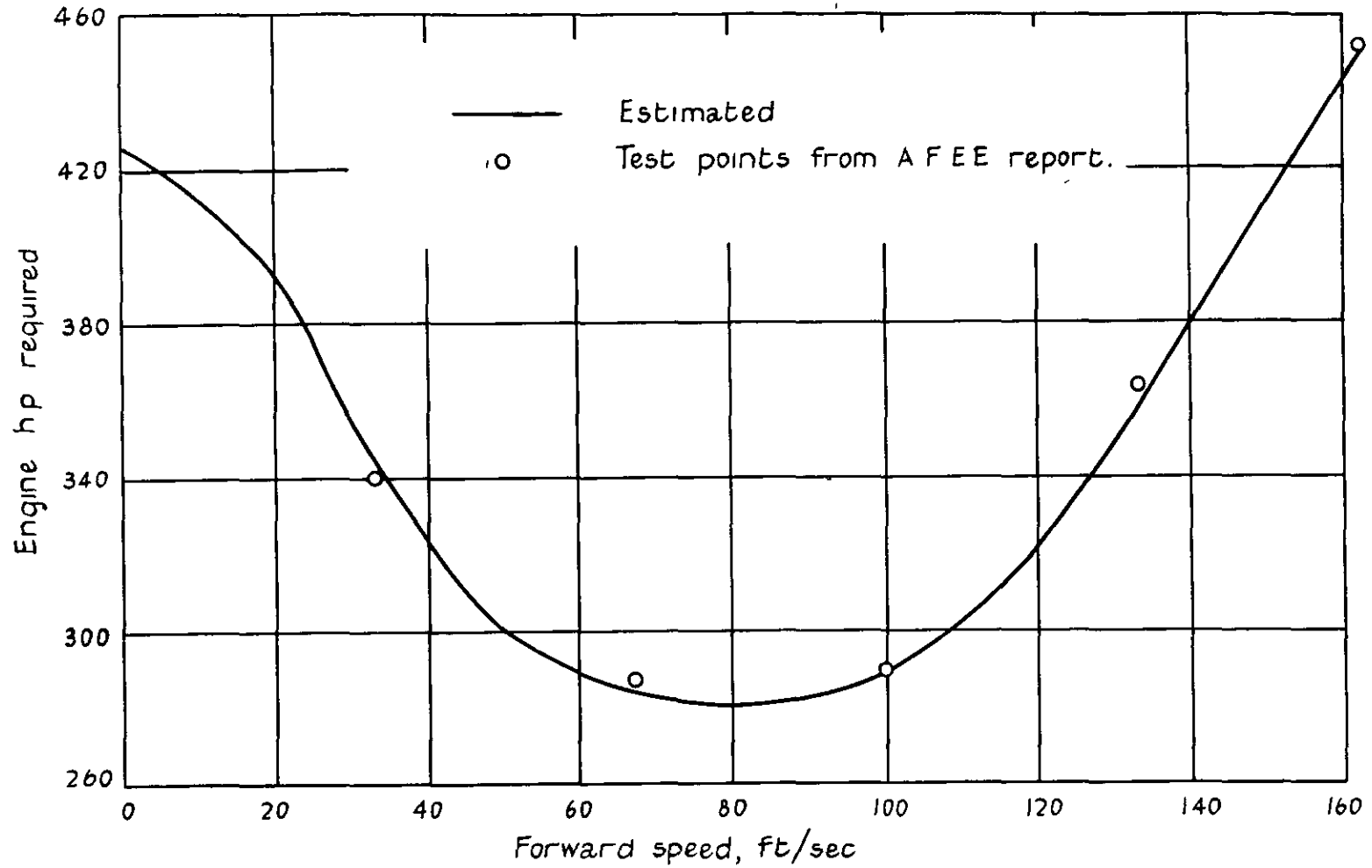
Variation in effective mean blade drag coefficient
after onset of tip stalling.
(f)_s as function of retreating tip angle of attack

FIG 13



Induced power correction factor $(f)_i$ against $\frac{V}{\sqrt{w}}$,

showing departure from $(f)_i = \frac{13.85 \sqrt{w}}{V}$ at low forward speeds.

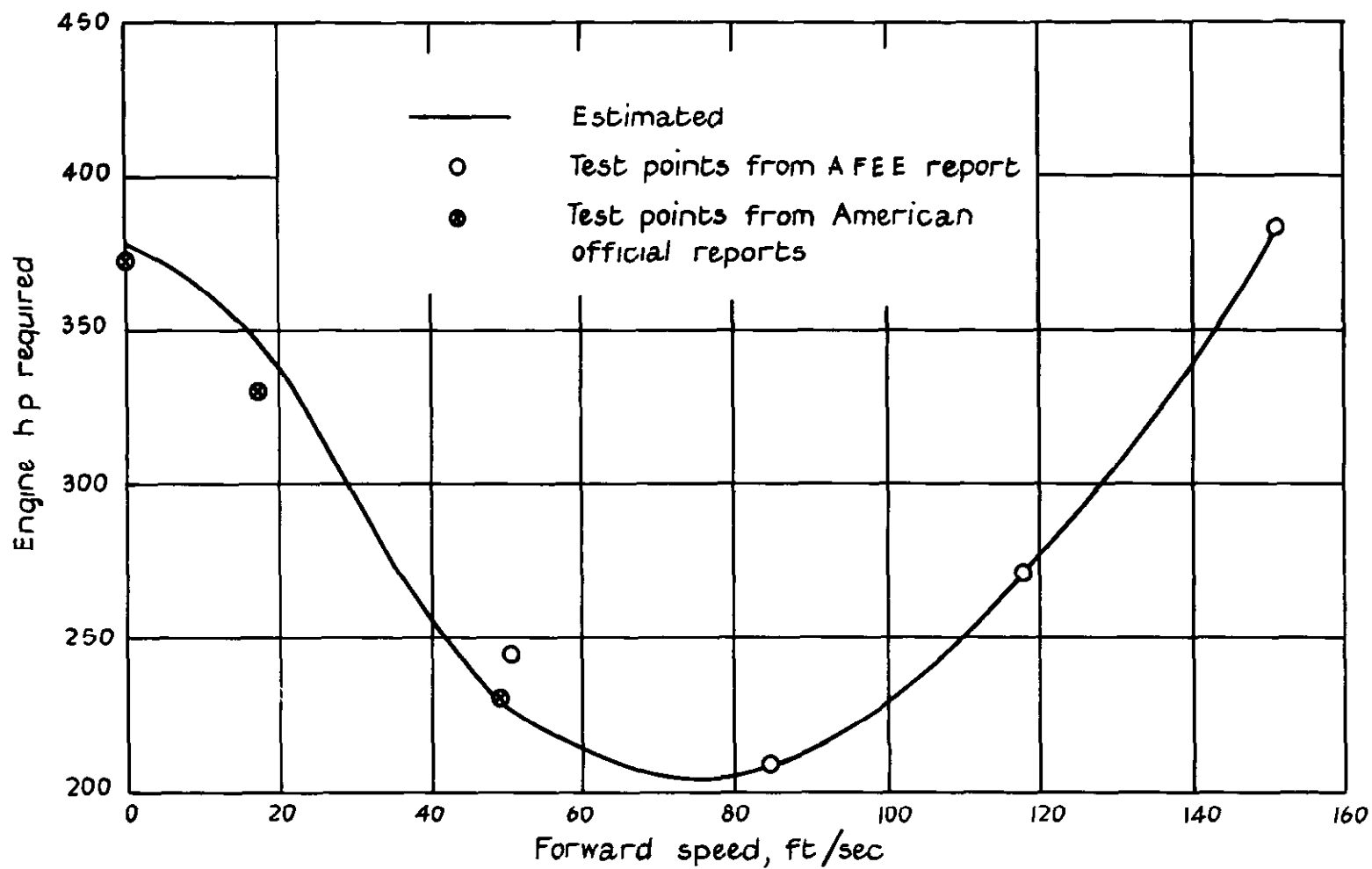


Bristol type 171 Mk 1

Level speed performance at 500 ft

Weight 4750 lb, ΩR 656 ft/sec

FIG 14



Sikorsky S 51.

Level speed performance at 1000 ft.

Weight 4850 lb ΩR 485 ft/sec

FIG. 15.

Fig 16

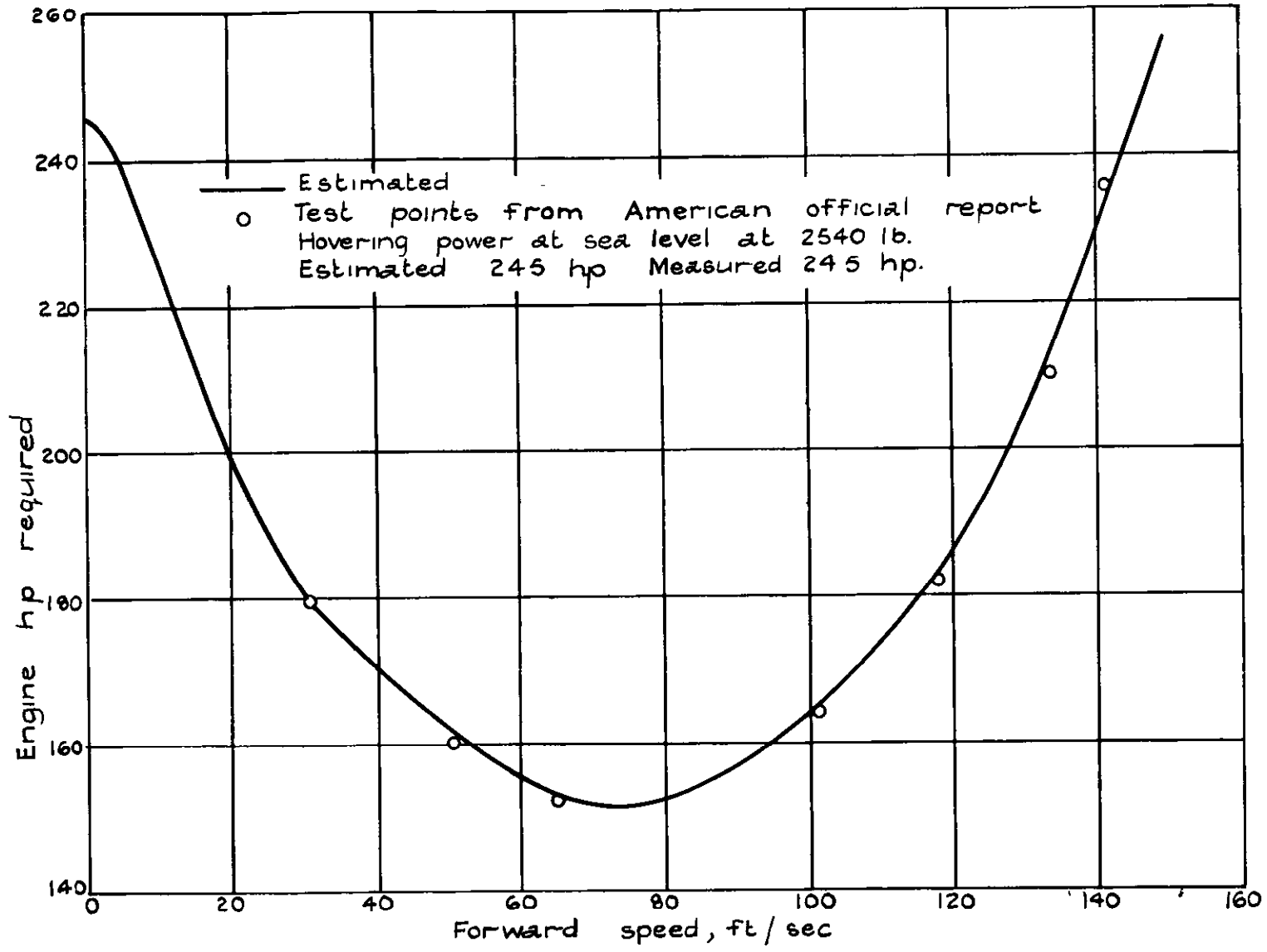


FIG 16

Sikorsky YH - 18A (service version of S52) Level speed performance at 3000 ft
Weight 2480 lb, diameter 33 ft, ΩR 562 ft/sec

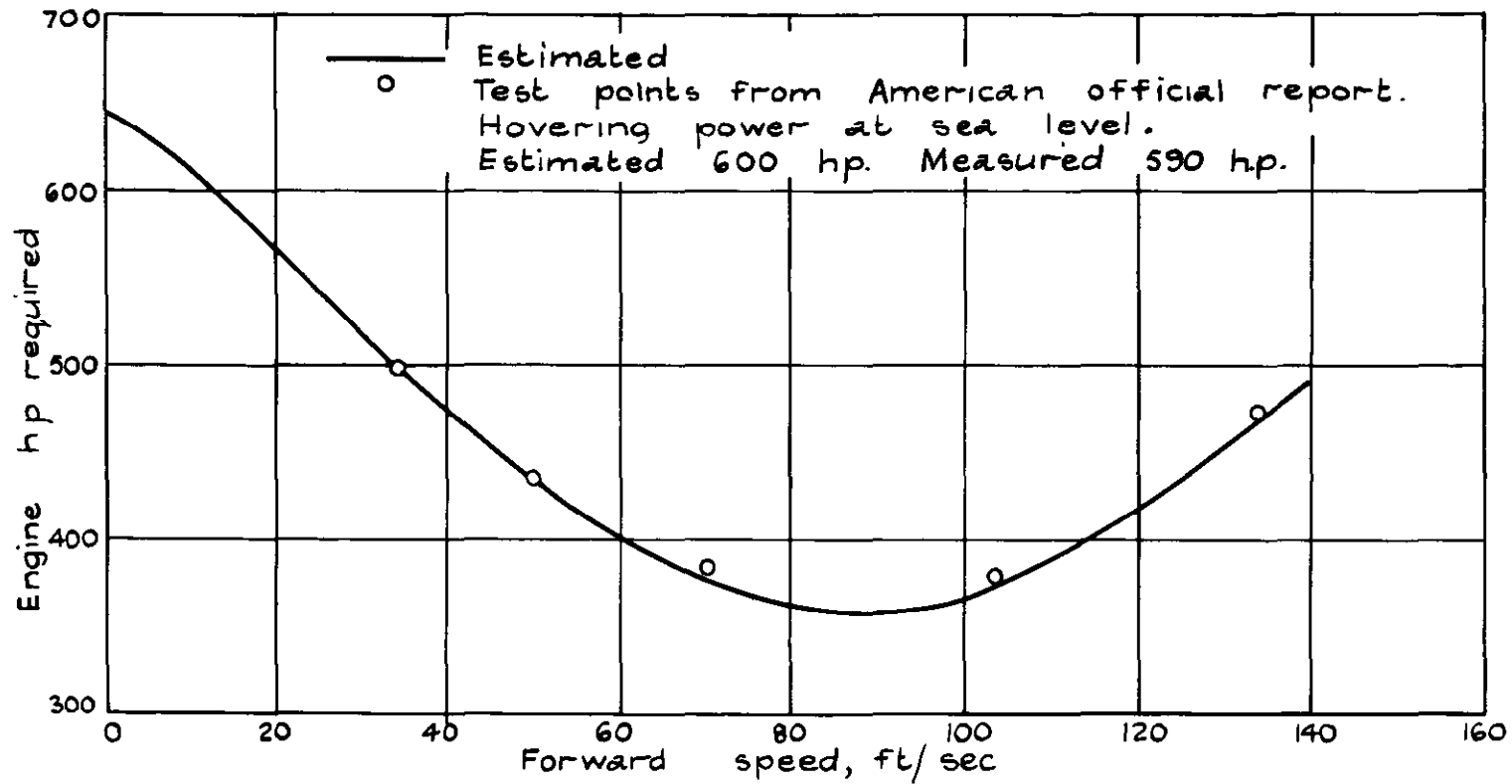
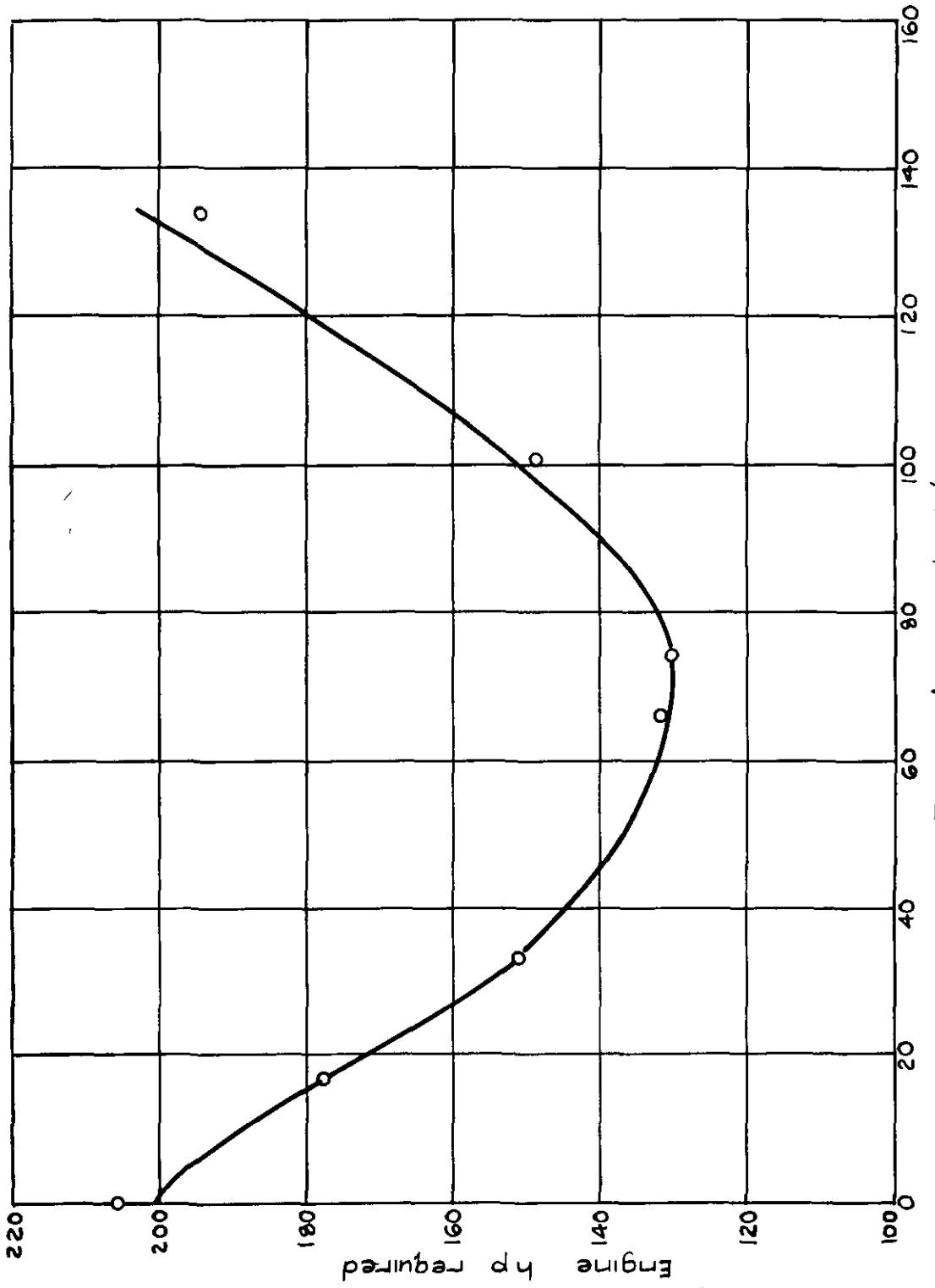


FIG 17.

Type A. Level speed performance at 7500ft. Single two bladed main rotor, diameter 47.5ft. Tail rotor. Weight 6284 lb, ΩR 695 ft/sec.

FIG 18.



Type B Level speed performance at 1500ft Single two bladed main rotor,
diameter 35 ft Weight 2350 lb, ΩR 630 ft/sec.

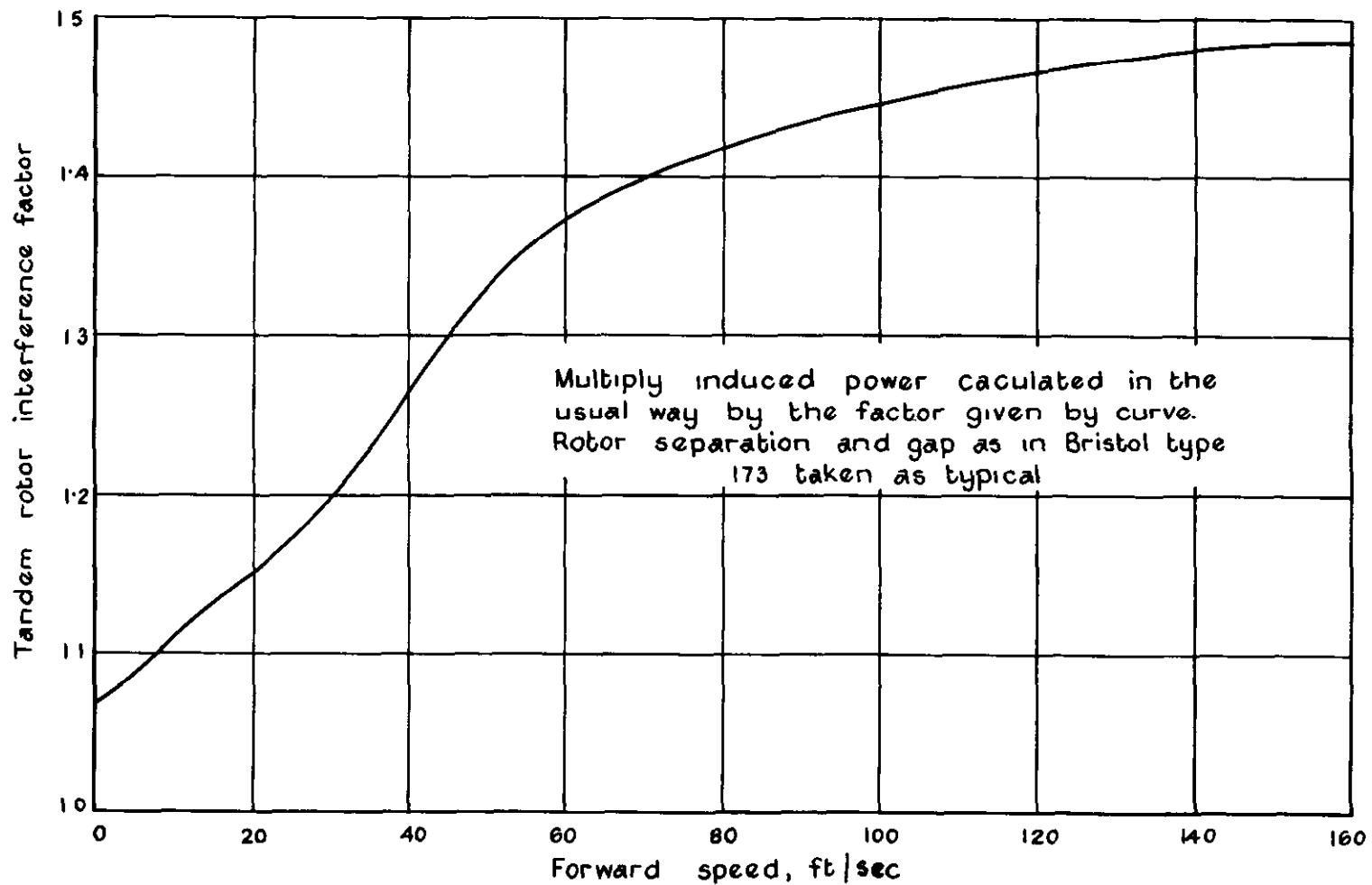
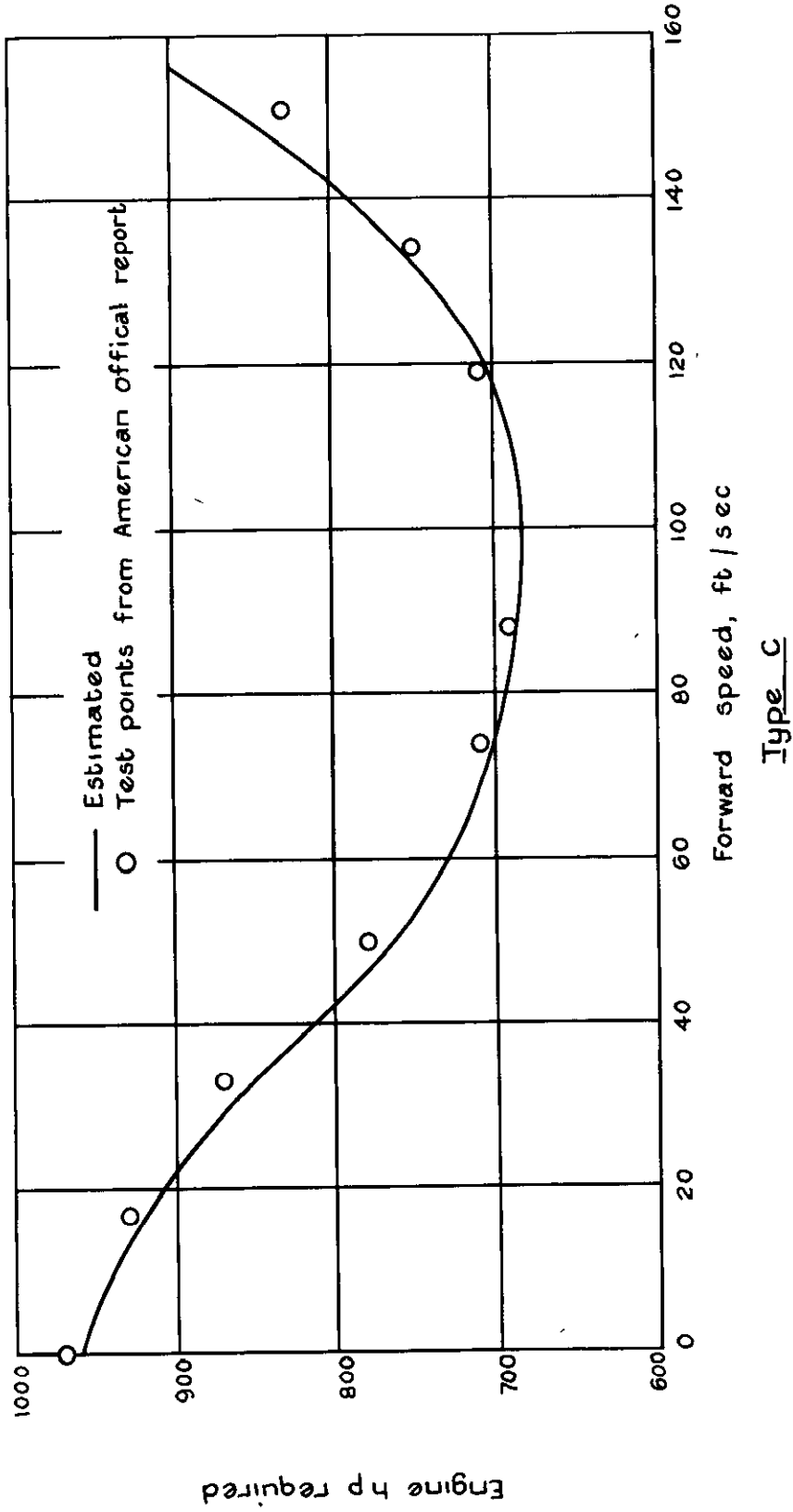


FIG. 19

Inter rotor interference factor. Tandem rotors.

FIG.20



Tandem rotor, two 3 bladed rotors each 44ft diameter. Weight 10850 lb
 ΩR 595ft/sec Level speed performance at sea level.

C.P. No. 183

(16,578)

A R C Technical Report

CROWN COPYRIGHT RESERVED

PRINTED AND PUBLISHED BY HER MAJESTY'S STATIONERY OFFICE

To be purchased from

York House, Kingsway, LONDON, W.C.2 423 Oxford Street, LONDON, W.1

P.O. Box 569, LONDON, S.E.1

131 Castle Street, EDINBURGH, 2 1 St Andrew's Crescent, CARDIFF

39 King Street, MANCHESTER, 2 Tower Lane, BRISTOL, 1

2 Edmund Street, BIRMINGHAM, 80 Chichester Street, BELFAST

or from any Bookseller

1954

Price 6s 0d net

PRINTED IN GREAT BRITAIN



S.O. Code No 23-9007-83

C.P. No. 183